PREDICTION OF MARTENSITE VOLUME FRACTION IN MULTI-COMPONENT DUAL PHASE STEELS

82868

A Thesis Submitted
In Partial Fulfilment of the Requirements
for the Degree of

MASTER OF TECHNOLOGY

By

KULVIR SINGH

to the

DEPARTMENT OF METALLURGICAL ENGINEERING

INDIAN INSTITUTE OF TECHNOLOGY KANPUR

AUGUST, 1983

POST GRADUATE OFFICE
Submitted on. 26.8.83

Certificate

This is to certify that the work presented in this thesis entitled "Prediction of Martensite Volume Fraction in Multi-Component Dual Phase Steels" by Mr. Kulvir Singh has been carried out under my supervision and it has not been submitted elsewhere for a degree.

August, 1983.

R.C. Sharma
Assistant Professor
Department of Metallurgical Engineering
Indian Institute of Technology
Kanpur

28 MAY 1994

CENTRAL LIBRARY
I. I. T. Kanpur
Acc. No. A 82544

Acknowledgement

I take this opportunity to express my sincere gratitude to Dr. R.C. Sharma for his invaluable guidance and suggestions throughout the course of this work.

I am highly indebted to Prof. A. Ghosh for providing process metallurgy laboratory facilities for the completion of my experimental work.

The help and co-operation rendered by Mr. G.S. Sharma, Mr. Malhotra, Mr. K.P. Mukherjee, Mr. A. Pal and Mr. H.C. Srivastava throughout the course of this work are greatly acknowledged.

I would like to thank Mr. R.N. Srivastava for the excellent typing and Mr. B.K. Jain for the beautiful tracing of the figures.

I am highly indebted to all my friends who have made my stay here lively and flamboyant. Especially I am extremely thankful to Mr. S.K. Tewari, Mr. Y. Ravishankar, Mr. A. Majumdar, Mr. Rajiv Sharma, Mr. R.K. Sharma and Mr. P.K. Subramaniam who have helped me when I needed them most.

At last but not least, my sincere thanks are also due to Miss Suman Chauhan for her constant inspirations at the critical stages of this work.

Kanpur
August, 1983.

- Kulvir Singh

Contents

Chapter			Page
List of Tables			v
List of Figures			vi
Synopsis			vii
1.	Introduction		1
2.	Literature Review		5
	2.1	Formation of Austenite	5
	2.2	Ferrite Formation or Austenite Decomposition	7
		2.2.1 Theory of Partitioning	9
		2.2.2 Para-Equilibrium	10
		2.2.3 Local Equilibrium No-Partition	10
	2.3	High Supersaturation Region	11
3.	Calculation of the Austenite Volume Fraction		13
	3.1	Thermodynamic Model	13
	3.2	Solution of the System of Thermodynamic Equations for the Volume Fraction of Austenite	16
		3.2.1 In Complete Equilibrium	16
		3.2.2 In Local Equilibrium	22
4.	Results and Discussion		26
5.	Experimental Studies		29
	5.1	Introduction	29
	5.2	Materials	29
	5.3	Heat Treatment	29
		5.3.1 Decarburisation and Oxidation	29
		5.3.2 Heat Treatment Processes	30
	5.4	Metallography	31
	5.5	Results and Discussion	31
6.	Conclusions		33
References			34
Appendix I			
Appendix II			
Appendix III			
Appendix IV			

List of Tables

No.	Title	Page
3.1	Interaction parameters	37
3.2	Free energy change $\Delta^{o}G^{\alpha-\gamma}$ for standard state at infinite dilution	38
3.3	Tabulated values of free energy change for iron	39
4.1	Chemical composition and calculated Ae_3 temperatures of the steels	41
4.2	Volume fractions of martensite	42
4.3	Mole fractions of ferrite and martensite in complete equilibrium	44
4.4	Mole fractions of ferrite and martensite in local equilibrium no-partition	47
5.1	Salt bath composition	50
5.2a	Measured volume fractions of martensite (intermediate quenching)	50
5.2b	Measured volume fractions of martensite (intermediate normalising)	50

List of Figures

No.	Title	Page
2.1	Schematic diagrams of three steps in austenite growth during intercritical annealing of ferrite-pearlite steels (1) Dissolution of pearlite, (2a) Austenite growth with carbon diffusion in austenite, (2b) Austenite growth with manganese diffusion in ferrite, and (3) Final equilibration with manganese diffusion in austenite	51
2.2	Austenite formation diagram for 0.12 C-1.5 Mn Steel	52
2.3	Equilibrium and local equilibrium no-partition boundaries at 960°K	53
2.4	Schematic penetration curves for carbon and manganese during the ferrite growth by LENP mechanism	54
2.5	Schematic representation of regions where the no-partition reactions by PE and LENP mechanisms is feasible	55
4.1	V_m observed vs. V_m calculated	56
4.2	V_m observed vs. V_m calculated	57
4.3	V_m observed vs. V_{ml} calculated	58
5.1	Formation of martensite in 0.22 C-1.4 Mn steel during intermediate quenching	59
5.2	Formation of martensite in 0.22 C-1.4 Mn steel during intermediate normalising	60
5.3	Micrographs of 0.22 C-1.4 Mn steel intercritically annealed at 720°C for (a) 5 s, (b) 1 m, (c) 2 m, (d) 5 m and (e) 10 m	61

Synopsis

The computer programmes have been developed to calculate the martensite volume fractions of the dual phase steels in complete equilibrium and local equilibrium no-partition conditions. A large number of steels, for which the experimental martensite volume fraction values are available in the literature, are chosen to test our predictive methods. The predicted values show a good overall correlation with the observed values. The agreement between the observed and the predicted values is better with local equilibrium no-partition calculations at lower martensite volume fractions. But at higher volume fractions the agreement is better with the complete equilibrium values. The calculated martensite volume fraction values on the basis of the observed values rationalise the existing theories of the ferrite transformations.

A 0.22 C-1.4 Mn steel has been studied for the martensite volume fraction values. It exhibits that the martensite volume fraction increases as a function of intercritical annealing temperature and time and tends towards equilibrium for higher intercritical annealing times. Our observations do not predict the mechanism of transformation as the holding times at intercritical temperature were not sufficient to maintain the complete equilibrium. However, the martensite volume fraction values are almost equal formed by both intermediate quenching and intermediate normalising methods.

Chapter 1

Introduction

Dual phase steel was originally suggested by Rashid[1] and is currently a material of commercial interest for automotive applications. This interest originates from the demand for lighter more fuel efficient vehicles. For this very reason General Motors[2] have recently introduced these steels for the manufacture of the components of their vehicles. The total weight saving[3] is estimated about 18% of the component's weight. Dual phase steels combine high strength of conventional steels with good formability; approaching that of plain carbon steels. Dual phase steels,[3] so-called because they essentially consist of a dispersion of martensite in a ferrite matrix, are produced by intercritically annealing (usually in a continuous annealing furnace) and cooling at such a rate as to give the desired structure. These steels contain low carbon (C around 0.1%) with or without the micro-alloy additions. Although multiphase steels[4] have been the subject of intermittant research for decades, dual phase steels developed in their present form are quite recent and their development can be traced back to the work of Grange[5]. He showed that the creation of martensite in a ferrite matrix after quenching from an intercritical annealing temperature resulted in a material with reduced YS/UTS ratio and considerably improved uniform elongation. Later investigations by Matsuoka and Yamamori[6] and others supported the

results of Grange, and further showed that ferrite martensite dual-phase steels have high work hardening rates and improved UTS-elongation combination. To the first approximation the strength of the dual phase steels can be written as[7]

$$\sigma_c = \sigma_m \cdot V_m + \sigma_\alpha (1 - V_m)$$

where σ_m and σ_α are the strength of martensite and ferrite and V_m and $(1 - V_m)$ are their respective volume fractions. In general, the ductility also follows the same relationship, but in an inverse manner to that for strength. But recently Rizk and Bourell[8] have modified this relationship to give

$$\sigma_c = V_f(\sigma_f + \sigma_{dm}) + V_m \cdot \sigma_m$$

where, the additional term σ_{dm} is the contribution to the yield strength of ferrite because of the additional dislocation distribution in the ferrite due to the martensite transformation. The addition of dislocation density term theoretically enhances the mechanical strength of dual phase steels by a factor that is a function of martensite volume fraction. The mechanical properties typical of, and desirable in, a dual phase steels include;

1. the absence of a yield point i.e., continuous yielding behaviour (Rashid[1])
2. a yielding stress lower than that of the other steels of comparable ultimate tensile strength (Davies[9])
3. a high initial work hardening (Davies[9] and Gerbase et al[10]
4. a high uniform elongation (Davies[9], Davies and Magee[3]).

The continuous yielding behaviour and the depressed yield stress are ascribed to residual stresses resulting from

the austenite to martensite transformation (although other explanations for this behaviour have been suggested by Gerbase et al[10]). The amount by which the yield stress is decreased, increases with martensite volume fraction at low volume fractions (less than 5%) with a low yield strength to ultimate tensile strength ratio being maintained to much larger volume fractions. The ultimate tensile strength increases with martensite volume fraction while the uniform elongation decreases with martensite volume fraction. As a result, the volume fraction of martensite in the steel must be selected to provide the optimal combination of these two properties. Typically this optimal volume fraction is between 10 to 20% (Araki et al[11]).

Dual phase steels can be produced in any of the following ways.[12]

(1) Continuous annealing of hot or cold rolled sheets

(2) Step quenching

(3) Intermediate quenching

(4) Intermediate normalising.

Continuous annealing results in a relatively high cooling rate (using gas or water quenching) and as a result lean to moderate alloy steel is used since a large amount of hardenability is not required to produce the desired martensite plus ferrite structure. The step quenching leads to the formation of ferrite islands from austenite during cooling to the intercritical temperature range. In the further step of cooling, the remaining austenite transforms to the martensite to yield the desired structure. Intermediate quenching

and normalising means the cooling of the steel from austenitising temperature in a quenchant and air respectively, thereafter, heating to intercritical range and cooling in a quenchant. Here, the dual phase structure is developed by formation of ferrite and austenite islands during heating from the starting structure of the martensite. Then on cooling, the austenite transforms to martensite resulting in a desired structure.

Properties of dual phase steels are function of the volume fraction of martensite. The amount of martensite in dual phase steels is approximately equal to the amount of austenite formed during the intercritical annealing. The objective of this work is to calculate the volume fraction of austenite formed during the intercritical annealing as a function of temperature and alloy composition. The prediction of the austenite volume fraction involves the calculation of the two phase ($\alpha + \gamma$) phase equilibria in multi-component steels.

Chapter 2

Literature Review

Dual phase steels are prepared employing the following methods:

(1) Continuous annealing of hot or cold rolled sheets

(2) Step quenching

(3) Intermediate quenching

(4) Intermediate normalising.

All of these methods involve austenite formation and thereafter, nucleation and growth of ferrite from austenite. Which occurs through the diffusion of carbon and alloying elements from one phase to another.

2.1 Formation of Austenite

The formation of austenite in completely pearlitic steel has been discussed by Speich et al[13] and Hillert et al.[14] However, the formation of austenite in the intercritical temperature range with a ferrite pearlite starting microstructure differs from these cases. In this situation, the austenite continues to grow after dissolution of the pearlite is complete.[15] This situation is the characteristic of that which exists during intercritical annealing of the most of the dual phase steel sheets. The various steps that may occur during the transformation of the ferrite-pearlite structure into a ferrite-austenite structure are shown schematically in Figure 2.1. The first step consists of nucleation of austenite at the ferrite/cementite interfaces in the

pearlite and the growth of austenite into pearlite until pearlite dissolution is complete. The nucleation of austenite occurs instantaneously with almost no nucleation barrier,[13] so that the nucleation of austenite is not considered to be a rate controlling factor. The rate of the growth of austenite in this step is controlled primarily by the rate of carbon diffusion in the austenite between adjacent pearlite-cementite lamellae, but may also be influenced by diffusion of substitutional elements at low temperatures.[14]

At the end of first step, a high carbon austenite is generated which, however, is not in equilibrium with ferrite. Subsequent growth of this austenite into the ferrite to achieve partial equilibrium with the ferrite constitutes a second step. The slower growth of austenite in this second step may be controlled either by carbon diffusion in the austenite as in step 2a in Figure 2.1, or by the alloying element diffusion in the ferrite as in step 2b. In the third and final step, very slow final equilibration of the ferrite and austenite is achieved by the alloying element diffusion through the austenite (the diffusion rate of manganese in austenite is about three orders of magnitude slower than that in ferrite).

Speich et al[15] have constructed a diagram for the austenite formation for the 0.12 C-1.5 Mn steel, which is shown in Figure 2.2. By referring to this diagram it is not only easy to establish the time for formation of various amounts of austenite but also to quickly recognize the controlling kinetic processes at each stage of austenite formation.

Such diagrams can be drawn for all steels by carrying out the growth kinetics studies of austenite formation for those steels.

2.2 Ferrite Formation or Austenite Decomposition

The effect of alloying elements on the austenite to proeutectoid ferrite transformation in the Fe-C-X alloys has been studied by many investigators. The result of both the experimental and theoretical examinations is the emergence of two distinguishable regimes which can be characterised by the presence or absence of partitioning of the substitutional alloying element.

In the Fe-C-X systems, where X is a substitutional alloying element, carbon diffuses much faster than alloying elements. Under such a condition the diffusion controlled austenite decomposition reaction can take place in two ways. In the first case, the alloying element is partitioned between the parent (austenite) phase and the product phase (phases). Such a reaction is called partition reaction. In this case, the reaction is slowed down considerably because of the relative slow diffusion of the alloying element involved. In the second case, the alloying element undergoes no long range diffusion and the ratio of the alloying element to iron remains the same in the product phase (or phases) as in the parent phase ($X_X^\alpha/X_{Fe}^\alpha = X_X^o/X_{Fe}^o$).[16] The reaction is then controlled by diffusion of carbon. An alloying element affects the reaction kinetics only through its thermodynamic influence on the driving force for the reaction. Such a

reaction is called no partition reaction. In general, the partitioning reaction must take place at low supersaturations while the no partition reaction must take place at high supersaturations. The actual temperature of the partition no-partition transition, if it exists, depends on the alloy system and composition.

There is considerable evidence in the literature for a partition no-partition transition. Bowman[17] in 1946 reported that no partitioning of molybdenum was detected during the formation of proeutectoid ferrite in a number of Fe-C-Mo alloys transformed between 650-750°C. Aaronson and Domain[18] have studied the partitioning of the alloying elements between austenite and proeutectoid ferrite (or bainite) in a number of Fe-C-X systems. They detected no partitioning of X between austenite and the proeutectoid ferrite during the initial stages of transformation at every temperature studied in the case of Si, Mo, Al, Cr and Cu steels. However, they observed partitioning of X between austenite and proeutectoid ferrite at the temperatures above an individually critical temperature in Mn and Ni steels.

Purdy et al[19] have studied the proeutectoid ferrite reaction in a number of Fe-C-Mn alloys and found zero partitioning of Mn at high supersaturations, while there was definite evidence of partitioning at low supersaturations. If the reaction in the high supersaturation, no-partition region is allowed to proceed for long times; the alloying elements will eventually partition towards the thermodynamic equilibrium values. This has been studied by Gilmour et al[20]

in the Fe-C-Mn system and by Sharma and Kirkaldy[21] in the Fe-C-Ni system for the proeutectoid reaction.

2.2.1 Theory of Partitioning

The theory of partitioning of alloying elements during the austenite to ferrite transformation has been extensively developed. Hultgren,[22] in 1951, first suggested that two types of ferrite could form during the isothermal decomposition of austenite in alloy steels. He noted that at relatively low supersaturations the rates of transformation were slow while at higher supersaturations they were much faster and that the high and low supersaturation data could in many cases be represented by separate C-curves, on the TTT diagrams. He proposed, therefore, that at low supersaturations the interface is in local equilibrium and the transformation required the equilibrium redistribution of the alloying elements. The ferrite produced under such conditions was called orthoferrite. At low temperatures, i.e., high supersaturations, the slow diffusing alloying elements could not redistribute and thus the transformation would proceed under carbon diffusion control, precipitating the ferrite of the same alloying content as the austenite. He called this non-equilibrium product, paraferrite. Since this early work it has been found that the double C-curve does not necessarily imply that the alloying element partitions in the region of the upper C-curve.[23] Other reasons for the double C-curve (or the 'bay' in the C-curve) found in certain alloy systems have been suggested.[23,24] However, the general conclusion of Hultgren, that during

proeutectoid ferrite reaction the alloying elements partition at relatively low supersaturations and not at higher supersaturations, remains valid.

2.2.2 Para-Equilibrium

Hillert[25] and Rudberg[26] have discussed the position of the para-equilibrium boundaries in ternary, Fe-C-X alloy systems in more detail. Hillert[25] has shown that the para-equilibrium tie line must satisfy the criterion that the para-equilibrium phase boundaries can be calculated from a knowledge of free energy surfaces. A true para-equilibrium tie line must satisfy the criterion that the chemical potential of the high mobility element (carbon) must be the same in both of the phases, austenite and ferrite, while the ratio of the alloying element to iron remains constant in both the phases ($X_X^\alpha / X_{Fe}^\alpha = X_X^\gamma / X_{Fe}^\gamma$). The para-equilibrium boundaries must lie within the thermodynamically stable two phase field. Gilmour et al,[27] Sharma and Kirkaldy[21] and Sharma et al[28] have calculated such para-equilibrium boundaries for the Fe-C-Mn, Fe-C-Ni and Fe-C-Cr systems from basic thermodynamic data.

2.2.3 Local Equilibrium No-Partition

Another way in which a no-partition reaction can occur is designated as the local equilibrium no-parition condition. This has been described by Kirkaldy,[29] Hillert and others. Under this condition the precipitating phase, during a diffusion controlled transformation in an Fe-C-X alloy, may have substantially the same alloying element

composition as the original austenite phase and still remain in complete chemical equilibrium at the interface.

Kirkaldy[29] published solutions to diffusion equations for transformation in ternary alloys assuming local equilibrium at the interface. Purdy et al[19] extended these solutions of the diffusion equations for the Fe-C-Mn system to show that at low supersaturations these solutionspredict manganese partition and low growth rates due to manganese diffusion control, while at higher supersaturations the manganese need not partition and the transformation would be controlled by carbon diffusion.

The position of this local equilibrium no-partition boundary in the ternary Fe-C-X phase diagrams has been further considered by Coates[30,31] and others. The construction of such a boundary is schematically shown in Figure 2.3. The intersection of the carbon component ($\frac{X_X}{X_{Fe}}$ = Constant line) from the ferrite end of a tie-line in the stable $\alpha + \gamma$ two phase field and the extrapolation of the carbon iso-activity line in austenite from the austenite end of the tie line define a point of partition no-partition boundary. The locus of such points divides the two phase ($\alpha + \gamma$) region into partition and no-partition regions. Figure 2.4 shows the concentration profiles during the diffusion transformation, γ to α in the Fe-C-Mn system.

2.3 High Supersaturation Region

In the high supersaturation no-partitioning range, the two no-partition criteria described above could exist,

which of these two possible conditions actually operate and under what circumstances has not been completely determined. However, the problem has been discussed by Coates[30,31] and others. The local equilibrium model, in general, looks more attractive because it postulates a thermodynamic equilibrium across the interface where the mobility of atoms, in general, is much higher than in the bulk. However, at high reaction rates or very early times, the alloying element diffusion profile (spike) width in front of the growing interface calculated according to the local equilibrium model approaches atomic dimensions or less.[30,31] In such a case the local equilibrium model becomes ambiguous, so the reaction may proceed under these conditions according to the para-equilibrium model. Figure 2.5 schematically shows the possible operative regions for the various conditions.

Chapter 3

Calculation of the Austenite Volume Fraction

3.1 Thermodynamic Model

Dual phase steels essentially consist of ferrite and martensite. But these two phases are not in equilibrium with each other. While the progenitor of martensite, namely, austenite happens to be in equilibrium with ferrite at the intercritical annealing temperature. Therefore, to calculate martensite volume fraction, an assumption is made here that the complete austenite transforms to the martensite of same composition. But concommitantly some austenite remains untransformed, which is also taken in account with martensite. Therefore, actually the volume fraction of austenite is calculated and taken equivalent to the martensite volume fraction.

Thermodynamically the partial molar free energies or chemical potentials of the alloying elements and the solvent iron are equal in the two phases in equilibrium, i.e. in ferrite (BCC) and austenite (FCC). Therefore analytically we have

$$\bar{G}_i^{\alpha} = \bar{G}_i^{\gamma} \qquad \text{for} \quad i = 0 \text{ to } 7 \tag{3.1}$$

Numerical symbols 0 to 7 stand for Fe, C, Mn, Si, Ni, Cr, Mo and Cu respectively. $\bar{G}_i^{\phi}$ is the partial molar free energy of the element i in the phase ϕ. More explicitly it can be written as

$$\bar{G}_i^{\phi} = {}^{o}G_i^{\phi} + RT \ln a_i^{\phi} \tag{3.2}$$

or, $$\bar{G}_i^{\phi} = {}^{o}G_i^{\phi} + RT \ln X_i^{\phi} \cdot \gamma_i^{\phi} \tag{3.3}$$

where, ${}^{o}G_i^{\phi}$ is the standard free energy, a_i^{ϕ} is the activity, X_i^{ϕ} is the mole fraction and γ_i^{ϕ} is the activity coefficient of the alloying element i in the phase ϕ.

Considering a system composed of solvent 0 and n alloying elements i (at low concentrations), the first order of Taylor expansion due to Wagner[32] applied to the logarithm of the activity coefficient of every element in the neighbourhood of $X_o = 1$ yields expressions of the type

$$\ln \gamma_i^{\phi} = \ln {}^{o}\gamma_i^{\phi} + \sum_{j=1}^{n} E_{ij}^{\phi} \cdot X_j^{\phi} \tag{3.4}$$

where X_j is again the mole fraction of the solute j, the coefficient $E_{ij} = \left(\frac{\partial \ln \gamma_i}{\partial X_j}\right)\Big|_{X_o = 1}$ is the interaction coefficient for the solute j and the solute i in a solution of 0 and γ_i^{ϕ} is the activity coefficient of solute i existing at infinite dilution in a solution of solvent 0. The Gibbs-Duhem relation can be used to express the activity coefficient of the solvent 0 in terms of the interaction parameters and mole fractions of the alloying elements.[33] The resulting expression is

$$\ln \gamma_o^{\phi} = -\frac{1}{2} \sum_{i=1,j=1}^{i=n,j=n} E_{ij}^{\phi} \cdot X_i^{\phi} \cdot X_j^{\phi} \tag{3.5}$$

which on rearrangement yields a solution for E_{ij}^{ϕ}. The interaction parameters have the important property that the Maxwell relation holds, so that the interchangeability of indices is valid,[34] viz.

$$E^{\phi}_{ij} = E^{\phi}_{ji} \tag{3.6}$$

For a standard state of all alloying elements i, i = 1 to 7 at infinite dilution the activity coefficient ${}^{o}\gamma^{\phi}_{i}$ is equal to unity and its logarithm is equal to zero; consequently we can rewrite equation (3.4) as

$$\ln \gamma^{\phi}_{i} = \sum_{j=1}^{n} E_{ij} \cdot X_j \tag{3.7}$$

These interaction parameters can be expressed as a linear $\frac{1}{T}$ relation if known at one temperature which are summarised in Table 3.1.

It is important to note that the data for the interaction parametersare available for the types E_{ii} (i.e. self interaction) for i = 1 to 7 and for both phases concerned, and E_{ij} (i.e. carbon-alloying element) for j = 1 to 7 and for austenite only. The latter coefficients are used also for the ferrite (BCC) phase, the error introduced by the assumption being small because the coefficients are multiplied by the very small concentrations of carbon in the ferrite. This is in accord with the practice used in previous publications.[21,27] All other parameters E_{ij} ($i \neq j \neq 1$) were set equal to zero as in earlier work.[35,21,27] These latter simplifications, however, do not affect our results because:

(a) The interaction of different substitutional elements should be smaller compared to those between metal-carbon.

(b) Due to the different signs of the interaction parameters, the interactions may very well cancel each other.

(c) Our experience with the volume fraction calculations showed that generally the interaction parameters affect the volume fractions very nominally. So the error introduced by not including the E_{ij} ($i \neq j \neq 1$) is of the same order as the experimental uncertainty in measuring the volume fractions.

The quantities ${}^{o}G_i^{\gamma} - {}^{o}G_i^{\gamma}$, which are expressed as $\Delta^{o}G_i^{\alpha-\gamma}$, can also be expressed as function of temperature (usually linear or linear logarithmic) as shown in Table 3.2. $\Delta^{o}G_{Fe}^{\alpha-\gamma}$ is calculated with the help of the tabulated values of free energy change (DSGFE) for solvent iron at different temperatures. The tabulated values for different temperatures are given in Table 3.3. The expression employed for the calculation of $\Delta^{o}G_{Fe}^{\alpha-\gamma}$ is:

$$\Delta^{o}G_{Fe}^{\alpha-\gamma} = \text{DSGFE(J-1)} + (\text{DSGFE(J)} - \text{DSGFE(J-1)}).(\text{T} - \text{TEMP(J-1)})/(\text{TEMP(J)} - \text{TEMP(J-1)}).$$

3.2 Solution of the System of Thermodynamic Equations for the Volume Fraction of Austenite

3.2.1 In Complete Equilibrium

In the earlier part of the present chapter, the thermodynamic equations required for the calculation of martensite volume fraction and elemental composition have been discussed. In addition the activity coefficients were expressed as functions of the interaction parameters and the mole fractions of the alloying elements. With the aid of data calculated from equations given in Tables 3.1 and 3.2,

we can now proceed to the solution of the thermodynamic and mass balance equations determining the martensite volume fraction and elemental composition of ferrite and martensite phases.

When an alloy of given composition is in complete equilibrium in the $(\alpha + \gamma)$ two phase region, then in addition to the thermodynamic equations (3.1), it must also satisfy the following mass balance equations[36]:

$$X_i^{\alpha} \cdot V^{\alpha} + X_i (1 - V^{\alpha}) = X_i^{o} \qquad \text{for} \quad i = 1 \text{ to } 7 \qquad (3.8)$$

where, V^{α} is the volume fraction of the ferrite phase in a dual phase steel. The volume fraction of austenite is $(1 - V^{\alpha})$. Equation (3.8) yields

$$X_i^{\alpha} = (X_i^{o} - X_i^{\alpha} \cdot V^{\alpha})/(1 - V^{\alpha}) \qquad \text{for} \quad i = 1 \text{ to } 7 \qquad (3.9)$$

This system of seven mass balance equations (3.9) and eight thermodynamic equations (3.1) consisting of 15 unknowns can now be simultaneously solved for the volume fraction, V^{α}, and the composition of the ferrite and austenite.

In terms of the non-zero interaction parameters we have the following analytic system of equations:

$$\frac{\Delta^{o}G_{o}^{\alpha-\gamma}}{RT} = \ln \frac{1 - \sum_{1}^{7} X_i^{\alpha}}{1 - \sum_{1}^{7} X_i} - X_1^{\alpha} \sum_{2}^{7} E_{1i} X_i^{\alpha} + X_i^{\gamma} \sum_{2}^{7} E_{1i} X_i^{\gamma}$$

$$- \frac{1}{2} \sum_{1}^{7} E_{ii} (X_i^{\alpha})^2 + \frac{1}{2} \sum_{1}^{7} E_{ii} (X_i^{\gamma})^2 \qquad (3.10)$$

$$\frac{\Delta^{o}G_1^{\alpha-\gamma}}{RT} = \ln \frac{X_1^{\alpha}}{X_1^{\gamma}} + \sum_{1}^{7} E_{1i}X_i^{\alpha} + \sum_{1}^{7} E_{1i}X_i^{\gamma} \qquad (3.11)$$

$$\frac{\Delta^{o}G_i^{\alpha-\gamma}}{RT} = \ln \frac{X_i^{\alpha}}{X_i^{\gamma}} + E_{ii}^{\alpha}X_i^{\alpha} + E_{1i}X_i^{\alpha} - E_{ii}^{\gamma}X_i^{\gamma} - E_{1i}X_i^{\gamma} \qquad (3.12)$$

Equations (3.9), (3.10), (3.11) and (3.12) can be rearranged as follows for our calculations:

$$X_i^{\gamma} \cdot \gamma_i^{\gamma} \cdot \mathrm{Exp}(A_i) - X_i^{\alpha} \cdot \gamma_i^{\alpha} = 0 \quad \text{for } i = 0 \text{ to } 7 \qquad (3.13)$$

and,

$$X_i^{\alpha} \cdot V^{\alpha} + X_i^{\gamma}(1 - V^{\alpha}) - X_i^{o} = 0 \quad \text{for } i = 1 \text{ to } 7 \qquad (3.14)$$

where, $A_i = \dfrac{\Delta^{o}G_i^{\alpha-\gamma}}{RT}$ for $i = 0$ to 7

Now, in total, we have got 15 simultaneous linear equations and 15 unknowns as V^{α} and X_i^{α}, X_i^{γ} $i = 1$ to 7. We can, therefore, solve it by expressing the X_i^{α} as functions of temperature T and X_i^{γ} as the original composition of the alloy and substituting these values in the final equation which contains the only unknown V^{α}. Since an exact analytical solution cannot be found out we have to employ numerical techniques. Here, we employed two methods to solve this system.

(1) By transferring all the terms to R.H.S. except X_i^{γ}, i = 0 to 7 the system of equations (3.10), (3.11), (3.12) can be rearranged as:

The coefficients E_{1i} are taken the same for the ferrite (alpha) and austenite (gamma) phases and consequently no α and γ designation is used with them.

$$X_1^{\gamma} = (1 - \sum_{2}^{7} X_i^{\gamma}) - (1 - \sum_{1}^{7} X_i^{\alpha}) . Exp[-(\frac{\Delta^{o}G_{o}^{\alpha-\gamma}}{RT} - X_1^{\gamma} \sum_{2}^{7} E_{1i}X_i^{\gamma} - \frac{1}{2} \sum_{1}^{7} E_{ii}^{\gamma}(X_i^{\gamma})^2 + X_1^{\alpha} \sum_{2}^{7} E_{1i}X_i^{\alpha} + \frac{1}{2} \sum_{1}^{7} E_{ii}^{\alpha}(X_i)^2)] \quad (3.15)$$

$$X_1^{\alpha} = X_1^{\gamma} . Exp(\frac{\Delta^{o}G_{1}^{\alpha-\gamma}}{RT} + \sum_{1}^{7} E_{1i}X_i^{\gamma} - \sum_{1}^{7} E_{1i}(X_i^{\alpha})) \quad (3.16)$$

$$X_i^{\alpha} = X_i^{\gamma} . Exp(\frac{\Delta^{o}G_{i}^{\alpha-\gamma}}{RT} + E_{ii}^{\gamma}X_i^{\gamma} + E_{1i}X_1^{\gamma} - E_{ii}^{\alpha}X_i^{\alpha} - E_{1i}X_1^{\alpha}) \quad (3.17)$$

Equation (3.17) is reduced to this form because interaction parameter of one alloying element on the other except carbon (i.e. $E_{ij} = E_{ji} = 0$ for $i \neq j \neq 1$) are taken to be zero.

Now by substitution method the equations (3.9), (3.15), (3.16) and (3.17) can be solved to yield ferrite volume fraction, V^{α}, and the elemental composition in both the phases. The computer programme is given in Appendix I.

But since this programme diverges for the carbon more than 0.12 wt % we have to find out other solution, which is valid for appreciable ranges of alloying element percentages.

(2) This programme converges for the varying percentages of the alloying elements. But the total alloy content should be less than 5.0 wt % because we are dealing with dilute solutions.

Here, we employ equations (3.13) and (3.14). These equations are solved with the help of a subroutine, for the solution of simultaneous linear equations, stored in the library of the computer system DEC 1090. The calling name of

the subroutine is F04AAF in NAG file. The computer programme is given in Appendix II.

Both of these programmes are valid[37] specifically for the C upto 0.77 wt %, Cu upto 2.7 wt %, Mn, Ni, Cr upto 4.0 wt %, Si upto 1.0 wt % and Mo upto 2.0 wt % except the carbon for the first programme which diverges beyond 0.12 wt % C.

To calculate equilibrium Ae_3 temperature equations (3.10), (3.11) and (3.12) can be employed. Where, the system contains 8 unknowns; X_i^α for i = 1 to 7 and T = Ae_3. We can, therefore, solve it by expressing the X_i^α as functions of temperature T and substituting in the 8th equation which contains only the unknown temperature T (= Ae_3). The original programme for equilibrium Ae_3 calculation is made by Kirkaldy and Baganis.[38] By transferring all the R.H.S. terms involving X_i^γ, i = 1 to 7, the system of equations (3.10), (3.11) and (3.12) can be rearranged as

$$\frac{\Delta^o G_o^{\alpha-\gamma}}{RT} + \ln(1 - \sum_1^7 X_i^\gamma) - X_1^\gamma \sum_2^7 E_{1i}X_i^\gamma - \frac{1}{2}\sum_1^7 E_{ii}^\alpha (X_i^\gamma)^2$$

$$= \ln(1 - \sum_1^7 X_i^\alpha) - X_1^\alpha \sum_2^7 E_{1i}X_i^\alpha - \frac{1}{2}\sum_1^7 E_{ii}^\alpha (X_i^\alpha)^2 \qquad (3.18)$$

$$\frac{\Delta^o G_1^{\alpha-\gamma}}{RT} + \ln(X_1^\gamma) + \sum_1^7 E_{1i}X_i^\gamma = \ln(X_1^\alpha) + \sum_1^7 E_{1i}X_i^\alpha \qquad (3.19)$$

and

$$\frac{\Delta^o G_i^{\alpha-\gamma}}{RT} + \ln(X_i^\gamma) + E_{ii}^\gamma X_1^\gamma + E_{1i}X_i^\gamma = \ln(X_i^\alpha) + E_{ii}^\alpha X_i^\alpha + E_{1i}X_1^\alpha$$

(3.20)

Since the X_i^{γ}, i = 1 to 7 represents the INPUTS to this programme. Equations (3.18), (3.19) and (3.20) can be written as

$$F_o(T, E, INPUT) = \ln(1 - \sum_{1}^{7} X_i^{\alpha}) - X_1^{\alpha} \sum_{2}^{7} E_{1i} X_i^{\alpha} - \frac{1}{2} \sum_{1}^{7} E_{ii}^{\alpha} (X_i^{\alpha})^2 \quad (3.21)$$

$$F_1(T, E, INPUT) = \ln(X_1^{\alpha}) + \sum_{1}^{7} E_{1i} X_i^{\alpha} \quad (3.22)$$

$$F_i(T, E, INPUT) = \ln(X_i^{\alpha}) + E_{ii}^{\alpha} X_i^{\alpha} + E_{1i} X_i^{\alpha} \quad (3.23)$$

In this form the system of equations can be solved by trial and error method. Starting from a trial temperature T_{tr} (1000°K or the one corresponding to plain Fe-C), equations (3.22) and (3.23) yield the seven unknowns X_i^{α}, i = 1 to 7, employing the algebraic transformation iteration scheme.[39] The numerical values of X_i^{α}, i = 1 to 7 thus obtained can be substituted in equation (3.21) which in the following form:

$$\phi(T) = F_o(T, INPUT) - \ln(1 - \sum_{1}^{7} X_i^{\alpha}) + X_i^{\alpha} \sum_{2}^{7} E_{1i} X_i^{\alpha} + \frac{1}{2} \sum_{1}^{7} E_{ii}^{\alpha} (X_i^{\alpha})^2 \quad (3.24)$$

is now a single function of T. Equation (3.24) can now, through Newton-Raphson technique,[40] give a better approximation T_{new}. The approximate T_{new} is now taken as trial temperature and the loop is repeated until the trial temperature and the derived one converge to the desired degree (usually within 1°K). This trial and error scheme usually

converges in less than 10 iterations. The computer programme is given in Appendix III.

3.2.2 In Local Equilibrium

When an alloy is cooled below the transformation temperature, it may transform with or without the partitioning of the alloying elements between the ferrite and the austenite. If it transforms without the partitioning of the alloying elements, but simultaneously maintaining the complete equilibrium between the two phases at the interface, then it is said to transform by local equilibrium as defined in the earlier chapter.

Under these conditions the volume fraction of the austenite obtained during the intercritical annealing would, in general, be different than the calculated above for the complete equilibrium. A separate programme has been developed to calculate the austenite volume fraction under the local equilibrium no-partition condition and is described below.

In the earlier part of this chapter, we have calculated the austenite volume fraction and elemental composition of ferrite and austenite phases in complete equilibrium condition. For calculating the tie line in local equilibrium condition we presume $X_i^{\gamma L} = X_i^{\alpha}$, i = 2 to 7 and $X_i^{\alpha L}$ as the original composition of the alloy steel. But $X_1^{\alpha L}$ is taken as X_1^{α} as the tie line passes through this point. In local equilibrium also the partial molar free energies or chemical potentials of the alloying elements and the solvent iron, at local equilibrium Ae_3 temperature T, are equal in two

phases. Therefore, equation (3.1) applies here too. Concomitantly, the ratio of the alloying element mole fraction to the mole fraction of solvent iron in the ferrite phase is constant, as it has been defined in previous chapter. This ratio equals to the ratio of alloying element mole fraction to the mole fraction of solvent iron in the original alloy steel. Therefore, we have

$$\frac{X_i^{\alpha}}{X_{Fe}^{\alpha}} = \frac{X_i^{o}}{X_{Fe}^{o}} \qquad \text{for} \quad i = 2 \text{ to } 7 \tag{3.25}$$

Now the equations (3.1) and (3.25) can be rearranged as:

$$X_1 = (1 - \sum_{2}^{7} X_i^{\gamma}) - (1 - \sum_{1}^{7} X_i^{\alpha}) \cdot \text{Exp}[-(\frac{\Delta^{o}G_{o}^{\alpha-\gamma}}{RT} - X_1^{\gamma} \sum_{2}^{7} E_{1i}X_i^{\gamma} - \frac{1}{2} \sum_{1}^{7} E_{ii}^{\gamma}(X_i^{\gamma})^2 + X_1^{\alpha} \sum_{2}^{7} E_{1i}X_{1i}^{\alpha} + \frac{1}{2} \sum_{1}^{7} E_{ij}^{\alpha}(X_i^{\alpha})^2)] \tag{3.26}$$

$$X_1^{\alpha} = X_1^{\gamma} \cdot \text{Exp}(\frac{\Delta^{o}G_1^{\alpha-\gamma}}{RT} + \sum_{1}^{7} E_{1i}X_i^{\gamma} - \sum_{1}^{7} E_{1i}X_i^{\alpha}) \tag{3.27}$$

$$X_i^{\gamma} = X_i^{\alpha} \cdot \text{Exp}[-(\frac{\Delta^{o}G_i^{\alpha-\gamma}}{RT} + E_{ii}^{\gamma}X_i^{\gamma} + E_{1i}X_1^{\gamma} - E_{ii}^{\alpha}X_i^{\alpha} - E_{1i}X_1^{\alpha}))] \qquad \text{for} \quad i = 2 \text{ to } 7 \tag{3.28}$$

$$\text{and,} \quad X_i^{\alpha} = \frac{X_i^{o}}{X_{Fe}^{o}} \cdot X_{Fe}^{\alpha} \qquad \text{for} \quad i = 2 \text{ to } 7 \tag{3.29}$$

Now, substituting our approximate mole fractions to the equations (3.26), (3.27), (3.28) and (3.29), this system of equations can be solved to yield the elemental composition of

the ferrite and the austenite phases. Further to calculate the composition in local equilibrium no-partition condition, we have to employ the carbon iso-activity line calculations. Along the carbon iso-activity line the activity of carbon remains unchanged. In this solution the ratio of the alloying element mole fraction to the mole fraction of the solvent iron remains constant. Therefore, we end up with the following equations:

$$A_c = X_1^{\gamma L} \cdot \mathrm{Exp}\left(\sum_{1}^{7} E_{1i} \cdot X_i^{\gamma L}\right) \quad \text{for} \quad i = 1 \text{ to } 7 \tag{3.30}$$

and,

$$\frac{X_i^{\gamma N}}{X_{Fe}^{\gamma N}} = \frac{X_i^{o}}{X_{Fe}^{o}} \quad \text{for} \quad i = 2 \text{ to } 7 \tag{3.31}$$

With the help of equation (3.30) the activity of carbon can be calculated and can be employed as such for calculating the new mole fractions in the austenite phase in local equilibrium no-partition condition. After rearrangement of equations (3.30) and (3.31) we have

$$X_1^{\gamma N} = A_c \cdot \exp\left[-\left(\sum_{1}^{7} E_{1i} \cdot X_i^{\gamma N}\right)\right] \tag{3.32}$$

$$X_i^{\gamma N} = \frac{X_i^{o}}{X_{Fe}^{o}} \cdot X_{Fe}^{\gamma N} \quad \text{for} \quad i = 2 \text{ to } 7 \tag{3.33}$$

where, $X_i^{\alpha L}$ and $X_i^{\gamma L}$ are the mole fractions of the alloying elements in the ferrite and the austenite phases in local equilibrium no-partition respectively. $X_i^{\gamma N}$ is the mole fraction of alloying elements in austenite phase in local

equilibrium no-partition employing the carbon iso-activity line calculations.

Equations (3.32) and (3.33) cannot give exact solution analytically. Therefore, we have to employ an algebraic transformation scheme, where we substitute $X_1^{\gamma N} = X_1^{\gamma L}$ and $X_i^{\gamma N} = X_i^{\alpha L}$ which is explicitly shown in Figure 2.3. By substituting these values we get next set of iterations which is again substituted in equations (3.32) and (3.33) till we get the new set of values converging to the desired accuracy in comparison to the earlier ones (in our case the accuracy is 0.000001). These sets of compositions in complete and local equilibrium no-partition give us the tie lines in the two equilibrium conditions.

To calculate the volume fraction of austenite in local equilibrium no-partition condition the following mass balance equation for carbon is employed:

$$X_1^{\alpha L} \cdot V^{\alpha L} + X_1^{\gamma N} (1 - V^{\alpha L}) = X_1^{o} \qquad (3.34)$$

A separate programme for local equilibrium no-partition calculations is given in Appendix IV.

Both of these programmes for complete and local equilibrium no-partition conditions can be used prolifically for the variety of steels limiting in the composition as defined in Section 3.2.1 of this chapter.

Chapter 4

Results and Discussion

A large number of steels, for which the experimental martensite volume fraction values are available in the literature, were chosen to test our predictive methods. The chemical compositions of these steels and their calculated Ae_3 temperatures are summarised in Table 4.1. The martensite volume fraction values for these steels, predicted on the basis of complete equilibrium and the local equilibrium no-partition are given in Table 4.2. Figures 4.1 and 4.2 show the plots between observed and the calculated (complete equilibrium) martensite volume fraction values for these steels and in Figure 4.3 the observed martensite volume fraction values are plotted against the values calculated by assuming local equilibrium no-partitioning. The calculated chemical compositions of ferrite and martensite in complete equilibrium and local equilibrium no-partition are also summarised in Tables 4.3 and 4.4.

The martensite volume fraction values calculated by both the methods show a good overall correlation with observed values as seen in Table 4.2 and Figures 4.1 and 4.3. For the observed martensite volume fraction values upto approximately 0.4, the agreement between the observed and the calculated values is better with local equilibrium no-partition calculations than the complete equilibrium calculations as seen in Figures 4.1 and 4.3. At higher

volume fractions the agreement seems to be better with the complete equilibrium values (Figure 4.2). In some cases (at higher volume fractions) the martensite volume fraction could not be calculated by the local equilibrium no-partition as the intercritical annealing temperatures for these steels were higher than the local equilibrium no-partition temperatures.

The austenite to ferrite transformation in the Fe-C-X systems from the supersaturated austenite has been studied by number of investigators.[18,19,21,30,31,44] In general, this transformation occurs by local equilibrium no-partition mechanism, below the LENP Ae_3 temperature. However, the partitioning of the alloying elements occurs on longer transformation times. The work of Wycliffe[43] show that also when a normalised steel is heated into the intercritical temperature range to obtain a dual phase steel, the reaction initially occurswithout any partitioning of the alloying elements and the partitioning starts only after longer annealing times. If the intercritical annealing temperature is higher than the LENP Ae_3 but lower than the equilibrium Ae_3, the transformation would occur with the partitioning of the alloying elements, however, this reaction is very slow. Hence, we would generally expect the martensite volume fraction values to be close to the local equilibrium no-partition calculations as is in fact observed for most of the steels (Figure 4.3). A situation close to complete equilibrium during the intercritical annealing may, however, be sometimes obtained when the annealing time is relatively

large and the structure is relatively fine. This is more likely when the starting grain size is very fine or the steel is heated to the intercritical temperature from the quenched (martensite) state. When a steel is heated into the intercritical temperature from the martensite structure, generally, a fine structure is observed. This is the situation for some of the steels, the observed volume fraction is between the LENP and the equilibrium calculations, quite a few of them being close to the complete equilibrium calculations.

In conclusion, for any steel of a given composition, the programmes given in the appendix may be used to calculate the expected martensite volume fractions. The LENP calculation gives the upper limit of the martensite volume fraction values and the complete equilibrium calculations the lower limit. Generally, the martensite volume fraction values would be expected to lie close to the LENP calculations. The conditions, under which the values close to the complete equilibrium will be obtained, have been mentioned above.

Chapter 5

Experimental Studies

5.1 Introduction

In the present work, a manganese steel was studied to observe its martensite volume fraction at different temperatures for different holding times at the intercritical temperature. The dual phase structure was obtained by employing intermediate quenching and intermediate normalising. The morphology of martensite formed on quenching from intercritical temperature is also studied as a function of temperature and time.

5.2 Materials

The 0.22 C and 1.40 Mn steel sheets of 10 mm thickness were cold rolled to 1.2 mm thickness with a reduction of 10-15% in each cycle. Then the specimens of 15 mm x 10 mm size were cut from these rolled sheets.

5.3 Heat Treatment

5.3.1 Decarburisation and Oxidation

Decarburisation and oxidation affect the microstructure of thin specimens quite significantly. Therefore, a great precaution is needed to check these undesirable effects.

Salt baths are widely used for the prevention of decarburisation and oxidation during heating of the specimens. Two different salt bath compositions are selected for

austenitizing and intercritical annealing treatments. The compositions of the salt baths are given in Table 5.1. Approximately 2% Borax is added to each bath. Borax releases its combined water in the form of steam on heating. This results in agitation of the bath and decreases in oxygen content of the bath. Graphite was also used to supplement the effect of Borax.

5.3.2 Heat Treatment Processes

Two methods were employed to develop the ferrite-martensite dual phase structure from the initial structure of ferrite + pearlite:

(1) Intermediate quenching

(2) Intermediate normalising.

(1) Intermediate quenching: All the specimenswere heated to 950°C and kept at this temperature for half an hour in the first salt bath for complete homogenisation and then directly quenched in water at room temperature. Thereafter, these specimens were again heated to 720, 740 and 760°C in the intercritical annealing temperature range in the second salt bath and held at these temperatures for the period of 5 s, 1 m, 2 m, 5 m and 10 m and subsequently quenched in water.

(2) Intermediate normalising: All the specimens were austenitised at 950°C for half an hour in the first salt bath and then cooled in air. Then the normalised samples were again heated to 720, 740 and 760°C for the periods of 5 s, 1 m, 2 m, 5 m and 10 m in the second salt bath and subsequently quenched in the water at room temperature.

5.4 Metallography

The treated specimens were tempered at 150°C for 2 Hrs, then polished and etched in Nital for microscopic studies.

All the specimens were observed under optical and scanning electron microscope. The micrographs were taken on ISI 60 scanning electron microscope.

Volume fraction measurements were carried out at different positions on the metallographic specimens. Systematic point count method was utilised for the measurement of point fraction which can be directly related to the volume fraction. Square lattice, containing 441 points, was used for the measurement of point fraction. Five measurements were made for each specimen and their mean was taken as the final value of volume fraction.

5.5 Results and Discussion

The martensite volume fraction values measured for the steel treated at different temperatures for different holding times are summarised in Table 5.2 and Figures 5.1 and 5.2.

The martensite volume fraction increases as the time for intercritical annealing is increased and is almost equal in intermediate quenching and intermediate normalising as seen in Table 5.2 and Figures 5.1 and 5.2. The mechanism of transformation cannot be predicted with the help of the calculated and the observed martensite fraction values as the time for intercritical annealing was not sufficient to

maintain the complete equilibrium. That is why the observed values of martensite volume fractions fall below the calculated values.

The formation of martensite on intercritically annealing at 720°C for different annealing times is as shown in Figure 5.3.

Chapter 6

Conclusions

(1) The computer programmes have been developed to calculate the expected martensite volume fraction values in dual phase steels based on complete equilibrium and local equilibrium no-partition condition.

(2) The observed martensite volume fraction values upto $\simeq$ 0.4; the agreement between the observed and the calculated values is better with local equilibrium no-partition calculations.

(3) At higher volume fractions the agreement is better with complete equilibrium calculations.

(4) The correlation between the observed and the calculated values has been rationalized on the basis of the theories of ferrite transformation in alloyed steels.

References

1. M.S. Rashid; SAE Paper 770211, 1977.

2. A.R. Marder; Met. Trans. A, Vol. 13A, 1982, p. 85.

3. R.G. Davies and C.L. Magee; In Structure and Properties of Dual Phase Steels, R.A. Kot and J.W. Morris, eds., AIME, New York, 1977, pp. 1-10.

4. T. Greday, H. Mathy and P. Messier; Ibid, p. 260.

5. R.A. Grange; In The Second International Conference on the Strength of Metals and Alloys 1970 Proceedings, Vol. III, ASM, 1970, pp. 861-876.

6. T. Matsuoka and K. Yamamori; Met. Trans., Vol. 6A, 1975, pp. 1613-1622.

7. G. Thomas and J.Y. Koo; In Structure and Properties of Dual Phase Steels, R.A. Kot and J.W. Morris, eds., AIME, New York, N.Y., 1979, pp. 183-201.

8. A. Rizk and D.L. Bourell; Scripta Met., Vol. 17, 1982, pp. 1321-1324.

9. R.G. Davies; Met. Trans., Vol. 9A, 1978, p. 41.

10. J. Gerbase, J.D. Embury and R.M. Hobbs; In Structure and Properties of Dual Phase Steels, R.A. Kot and J.W. Morris, eds., New York, N.Y., 1979, p. 118.

11. K. Araki, S. Fukunada and K. Uchida; Trans. I.S.I.J., Vol. 17, 1977, p. 701.

12. C.I. Garcia and A.J. Deardo; In Structure and Properties of Dual Phase Steels, R.A. Kot and J.W. Morris, eds., AIME, New York, N.Y., 1979, p. 40.

13. G.R. Speich and A. Szirmae; TMS-AIME, Vol. 245, 1969, pp. 1063-1074.

14. M. Hillert, K. Nilsson and L.B. Torndahl; J. Iron and Steel Institute, London, Vol. 209, 1971, p. 49.

15. G.R. Speich, V.A. Demarest and R.L. Miller; Met. Trans. A, Vol. 12A, 1981, pp. 1419-1428.

16. A.K. Shah; M.Tech. Thesis, Indian Institute of Technology, Kanpur (India), 1981.

17. F.E. Bowman; Trans. ASM, Vol. 36, 1946, p. 61.

18. H.I. Aaronson and H.A. Domain; Trans. TMS-AIME, Vol. 236, 1966, p. 781.

19. G.R. Purdy, D.H. Weichert and J.S. Kirkaldy; Trans. TMS-AIME, Vol. 230, 1964, p. 1025.

20. J.B. Gilmour, G.R. Purdy and J.S. Kirkaldy; Met. Trans., Vol. 3A, 1972, p. 3213.

21. R.C. Sharma and J.S. Kirkaldy; Can. Met. Quart., Vol. 12(4), 1973, p. 391.

22. A. Hultgren; Jernkout. Ann., Vol. 135, 1951, p. 403.

23. H.I. Aaronson; Trans. TMS-AIME, Vol. 224, 1962, p. 870.

24. R.C. Sharma and G.R. Purdy; Met. Trans., Vol. 5, 1974, p. 939.

25. M. Hillert; Jernkont. Ann., Vol. 136, 1952, p. 25.

26. E. Rudberg; Ibid, p. 91.

27. J.B. Gilmour, G.R. Purdy and J.S. Kirkaldy; Met. Trans., Vol. 3A, 1972, p. 1455.

28. R.C. Sharma, G.R. Purdy and J.S. Kirkaldy; Met. Trans., Vol. 10A, 1979, p. 1119.

29. J.S. Kirkaldy; Can. J. Phys., Vol. 36, 1958, p. 907.

30. D.E. Coates; Met. Trans., Vol. 3, 1972, p. 1203.

31. D.E. Coates; Met. Trans., Vol. 4, 1973, p. 2313.

32. C. Wagner; Thermodynamics of Alloys, Addison-Wesley, Reading, Mass., U.S.A., 1952, p. 51.

33. J.S. Kirkaldy and G.R. Purdy; Can. J. of Phys., Vol. 40, 1962, p. 202.

34. C.H.P. Lupis and J.F. Elliot; Acta Met., Vol. 14, 1966, p. 529.

35. G. Kirchner, H.Harvig and B. Urhenius; Met. Trans., Vol. 4, 1973, pp. 1059.

36. R.C. Sharma; Personal communication.

37. E.A. Baganis; M.S. Thesis, McMaster University, Hamilton, Ontario (Canada), 1976.

38. J.S. Kirkaldy and E.A. Baganis; Met. Trans. A, Vol. 9A, 1978, p. 495.

39. B. Carnahan, H.A. Luther and J.O. Wikes; Applied Numerical Methods, John Wiley and Sons. Inc., New York, N.Y., 1969, p. 168.

40. B. Carnahan; Ibid, p. 319.

41. E. Kreyszig; Advance Engineering Mathematics, Third edition, Wiley, 1972, p. 641.

42. G.S. Sharma; M.E. Thesis, University of Roorkee, Roorkee (India), 1982.

43. P.A. Wycliffe; Ph.D. Thesis, McMaster University, Hamilton, Ontario (Canada), 1981.

44. A.K. Shah and R.C. Sharma; Zeit. Metalkunde, Vol. 74, 1983, p. 394.

45. S.J. Barber; Metal Engg. Quart. ASM, 1963, p. 381.

Table 3.1 Interaction parameters[37]

S. No.	Interaction parameter	Expression
1	E^{γ}_{11}	8910.0/T
2	E^{γ}_{22}	-4950.0/T
3	E^{γ}_{33}	(-3.0590/T) - 41.0377 + 9.873 logT
4	E^{γ}_{44}	-1870.0/T
5	E^{γ}_{55}	330.0/T
6	E^{γ}_{66}	-2310.0/T
7	E^{γ}_{77}	-7260.0/T
8	E^{α}_{11}	0.0
9	E^{α}_{22}	-990.0/T
10	E^{α}_{33}	(-21787.0/T) + 6.4544 + 5.2320 logT
11	E^{α}_{44}	-1870.0/T
12	E^{α}_{55}	-2970.0/T
13	E^{α}_{66}	-4290.0/T
14	E^{α}_{77}	-8910.0/T
15	E_{21}	-4950.0/T
16	E_{31}	12650.0/T
17	E_{41}	5170.0/T
18	E_{51}	-14080.0/T
19	E_{61}	-10670.0/T
20	E_{71}	4180.0/T

Table 3.2 Free energy change $\Delta^{o}G^{\alpha-\gamma}$ for standard state at infinite dilution[38]

S. No.	Free energy change	Expression (J/mole)
1	$\Delta^{o}G_1^{\alpha-\gamma}$	-64111.4 + 32.158T
2	$\Delta^{o}G_2^{\alpha-\gamma}$	$-162318.2 + 259.981T - 0.1067T^2$
3	$\Delta^{o}G_3^{\alpha-\gamma}$	-24953.4 + 162.335T - 19.7669T lnT
4	$\Delta^{o}G_4^{\alpha-\gamma}$	-19016.3 + 13.527T
5	$\Delta^{o}G_5^{\alpha-\gamma}$	-1535.5 - 19.481T + 2.7481T lnT
6	$\Delta^{o}G_6^{\alpha-\gamma}$	2364.0 + 0.63T
7	$\Delta^{o}G_7^{\alpha-\gamma}$	$-106692.0 + 172.310T - 0.071T^2$

T in °K and $\Delta^{o}G^{\alpha-\gamma}$ in J/mole.

Table 3.3

Tabulated values of free energy change for iron [37]

Temperature (degs K)	free energy change
750.0	412.50
760.0	396.10
770.0	379.90
780.0	364.00
790.0	348.40
800.0	333.00
810.0	317.80
820.0	302.80
830.0	288.10
840.0	273.50
850.0	259.10
860.0	244.70
870.0	230.80
880.0	217.30
890.0	204.10
900.0	191.10
910.0	178.30
920.0	166.00
930.0	154.10
940.0	142.40
950.0	131.00
960.0	119.90
970.0	109.30
980.0	99.30
990.0	89.80
1000.0	80.80
1010.0	72.18
1020.0	64.16
1030.0	56.75
1040.0	50.15

Table 3.3 continued

1050.0	44.31
1060.0	39.11
1070.0	34.21
1080.0	29.92
1090.0	26.07
1100.0	22.22
1110.0	18.37
1120.0	14.92
1130.0	11.84
1140.0	9.10
1150.0	6.66
1160.0	4.48
1170.0	2.52
1180.0	0.74
1184.5	0.00
1190.0	-0.89
1200.0	-2.40
1210.0	-3.82
1220.0	-5.15
1230.0	-6.39
1240.0	-7.55
1250.0	-8.63
1260.0	-9.63
1270.0	-10.55
1280.0	-11.40
1290.0	-12.17
1300.0	-12.87

Table 4.1

Chemical composition and calculated Ae3 temperature of the steels

No. of steels	C	Mn	Si	Ni	Cr	Mo	Cu	Ae3 (Deg K)	ref
1	0.01	1.45	.004	0.0	0.0	0.0	0.0	1121.2	12
2	0.05	1.50	0.01	0.0	0.0	0.0	0.0	1107.2	12
3	0.15	1.50	0.01	0.0	0.0	0.0	0.0	1078.2	12
4	0.22	1.55	0.01	0.0	0.0	0.0	0.0	1051.9	12
5	.005	1.51	0.24	0.0	0.0	0.0	0.0	1128.1	15
6	0.06	1.47	0.23	0.0	0.0	0.0	0.0	1110.1	15
7	0.12	1.47	0.24	0.0	0.0	0.0	0.0	1093.1	15
8	0.16	1.53	0.24	0.0	0.0	0.0	0.0	1079.8	15
9	0.20	1.53	0.25	0.0	0.0	0.0	0.0	1069.8	15
10	0.29	1.51	0.23	0.0	0.0	0.0	0.0	1050.8	15
11	0.11	0.50	0.30	0.0	0.0	0.0	0.0	1125.7	10
12	0.12	1.50	0.65	0.0	0.0	0.0	0.0	1101.3	10
13	0.22	1.40	0.00	0.0	0.0	0.0	0.0	1064.5	42
14	0.06	0.32	0.00	0.0	0.0	0.0	0.0	1133.9	42
15	0.10	0.38	0.00	0.0	0.0	0.0	0.0	1124.6	42
16	0.08	1.00	0.00	0.0	0.0	0.0	0.0	1112.6	43
17	0.04	1.50	0.00	0.0	0.0	0.0	0.0	1109.8	43
18	0.04	1.00	0.00	0.0	0.0	0.0	0.0	1125.9	43
19	0.08	0.00	0.00	1.0	0.0	0.0	0.0	1118.6	43
20	0.08	0.00	1.00	0.0	0.0	0.0	0.0	1193.6	43
21	0.08	1.00	1.00	0.0	0.0	0.0	0.0	1156.1	43
22	.056	0.97	0.00	0.0	0.0	0.0	0.0	1121.1	43
23	.079	0.99	0.00	0.0	0.0	0.0	0.0	1113.2	43
24	0.30	0.97	0.00	0.0	0.0	0.0	0.0	1057.4	43
25	0.20	1.50	0.00	0.0	0.0	0.0	0.0	1066.5	43
26	0.12	1.50	0.00	0.0	0.0	0.0	0.0	1087.0	43

Table 4.2

Volume fractions of martensite

No. of Specimens	T_s	$V_{\alpha'}$	$V_{\alpha'}$ observed
	973	0.01369	0.017
	973	0.11940	0.096
	973	0.29870	0.275
	973	0.41950	**	0.415
	1033	0.02057	0.11834	0.015
	1033	0.01016	0.03672	0.003
	1013	0.00107	0.01073	0.000
	1053	0.32643	**	0.324
	1033	0.27731	0.60108	0.3005
	1013	0.10529	0.36042	0.2696
	1053	0.52716	**	0.514
	1033	0.39248	**	0.4117
	1013	0.29458	0.78973	0.3612
	1053	0.60860	**	0.595
	1033	0.50260	**	0.461
	1013	0.38052	**	0.4463
	1053	0.78298	**	0.659
	1033	0.59402	**	0.5541
	1013	0.45247	**	0.5256
	1053	0.97120	**	0.882
	1033	0.78506	**	0.5928
	1013	0.60267	**	0.624
	1003	0.13533	0.17781	0.150
	1003	0.24366	0.81645	0.170
	1003	0.41608	0.98692	0.410
	993	0.36862	0.84503	0.355
	983	0.32926	0.74531	0.310
	973	0.29620	0.67366	0.250
	1033	0.62749	**	0.554
	1013	0.47404	**	0.456

		.13771	0.15565	0.165
		0.11811	0.13573	0.156
		0.10228	0.11914	0.139
		0.08821	0.10544	0.125
		0.07856	0.09433	0.120
		0.06978	0.08513	0.100
		0.06245	0.07747	0.088
		0.10327	0.21038	0.235
		0.15930	0.18330	0.2075
		0.13747	0.16083	0.170
		0.12021	0.14243	0.130
		0.10611	0.12711	0.150
		0.09444	0.11507	0.135
		0.08465	0.10473	0.105
		0.16402	0.25208	0.300
		0.14163	0.35594	0.310
		0.08721	0.11223	0.170
		0.13698	0.16260	0.160
		0.08783	**	0.110
		0.16156	0.42032	0.230
		0.14527	0.15164	0.142
		0.13055	0.24542	0.225
		0.61195	0.98101	0.750
		0.45617	**	0.590
		0.30528	0.84664	0.390

Vc : the volume fraction of martensite in corplete equilibrium

Vcl: the volume fraction of martensite in local equilibrium

Vc observed: the volume fraction of martensite in complete equilibrium observed by different investigators

** : Vcl is more than 1.0

[illegible]	1033	.137711	0.15586	0.165
[illegible]	1023	0.11811	0.13579	0.156
[illegible]	1013	0.10228	0.11914	0.139
[illegible]	1003	0.08921	0.10544	0.125
[illegible]	993	0.07856	0.09430	0.120
[illegible]	983	0.06978	0.08513	0.100
[illegible]	973	0.06245	0.07747	0.090
[illegible]	1033	0.18327	0.21038	0.235
[illegible]	1023	0.15830	0.18330	0.2075
[illegible]	1013	0.13747	0.16089	0.170
[illegible]	1003	0.12021	0.14243	0.130
[illegible]	993	0.10611	0.12744	0.160
[illegible]	983	0.09444	0.11507	0.135
[illegible]	973	0.08465	0.10473	0.105
16	1023	0.18402	0.25208	0.300
17	1023	0.14463	0.35594	0.310
18	1023	0.08721	0.11223	0.170
19	1023	0.13698	0.16260	0.160
20	1023	0.08783	**	0.110
21	1023	0.16156	0.42032	0.230
22	1023	0.12527	0.16164	0.142
23	1023	0.18055	0.24542	0.225
24	1023	0.61195	0.98101	0.750
25	1013	0.45617	**	0.590
26	1013	0.30528	0.84664	0.390

Vm : The volume fraction of martensite in complete equilibrium

Vml: The volume fraction of martensite in local equilibrium

Vm observed: the volume fraction of martensite in complete equilibrium observed by different investigators

** : Vml is more than 1.0

Table 4.3

Mole fractions of ferrite and martensite in complete equilibrium

No. of steels	Phase	C	Mn	Si	Ni	Cr	Mo	Cu
1	F	.00028	.01436	.00008	-	-	-	-
	A	.01344	.04129	.00007	-	-	-	-
2	F	.00035	.01240	.00020	-	-	-	-
	A	.01691	.03615	.00017	-	-	-	-
3	F	.00048	.00948	.00020	-	-	-	-
	A	.02208	.02848	.00017	-	-	-	-
4	F	.00053	.00844	.00021	-	-	-	-
	A	.02381	.02583	.00017	-	-	-	-
5a	F	.00012	.01481	.00477	-	-	-	-
	A	.00385	.03140	.00412	-	-	-	-
b	F	.00017	.01510	.00476	-	-	-	-
	A	.00622	.03530	.00415	-	-	-	-
c	F	.00022	.01528	.00475	-	-	-	-
	A	.00936	.03991	.00419	-	-	-	-
6a	F	.00026	.01087	.00478	-	-	-	-
	A	.00821	.02350	.00404	-	-	-	-
b	F	.00030	.01131	.00471	-	-	-	-
	A	.01117	.02697	.00400	-	-	-	-
c	F	.00037	.01166	.00466	-	-	-	-
	A	.01499	.03109	.00399	-	-	-	-
7a	F	.00032	.00910	.00523	-	-	-	-
	A	.01021	.01998	.00429	-	-	-	-
b	F	.00037	.00952	.00508	-	-	-	-
	A	.01353	.02307	.00419	-	-	-	-
c	F	.00043	.00986	.00498	-	-	-	-
	A	.01779	.02676	.00414	-	-	-	-
8a	F	.00035	.00851	.00543	-	-	-	-
	A	.01086	.01885	.00438	-	-	-	-

Table 4.3 continued

5	F	.00068	.00273	-	-	-	-	-
	A	.02625	.00706	-	-	-	-	-
6	F	.00072	.00275	-	-	-	-	-
	A	.02986	.00754	-	-	-	-	-
7	F	.00076	.00276	-	-	-	-	-
	A	.03377	.00808	-	-	-	-	-
8	F	.00079	.00278	-	-	-	-	-
	A	.03790	.00868	-	-	-	-	-
9	F	.00081	.00278	-	-	-	-	-
	A	.04225	.00934	-	-	-	-	-
10	F	.00083	.00278	-	-	-	-	-
	A	.04683	.01007	-	-	-	-	-
15a	F	.00063	.00304	-	-	-	-	-
	A	.02243	.00745	-	-	-	-	-
5	F	.00067	.00307	-	-	-	-	-
	A	.02565	.00797	-	-	-	-	-
6	F	.00071	.00310	-	-	-	-	-
	A	.02920	.00853	-	-	-	-	-
7	F	.00075	.00312	-	-	-	-	-
	A	.03303	.00915	-	-	-	-	-
8	F	.00078	.00313	-	-	-	-	-
	A	.03707	.00983	-	-	-	-	-
9	F	.00080	.00314	-	-	-	-	-
	A	.04133	.01058	-	-	-	-	-
10	F	.00082	.01141	-	-	-	-	-
	A	.04581	.01141	-	-	-	-	-
16	F	.00047	.00788	-	-	-	-	-
	A	.01805	.02011	-	-	-	-	-
17	F	.00028	.01250	-	-	-	-	-
	A	.01115	.03127	-	-	-	-	-
18	F	.00042	.00894	-	-	-	-	-
	A	.01655	.02255	-	-	-	-	-
19	F	.00061	-	-	.00853	-	-	-
	A	.02321	-	-	.01548	-	-	-

Table 4.3 continued

20	F	.00086	-	.01997	-	-	-	-
	A	.03287	-	.01609	-	-	-	-
21	F	.00051	.00802	.02026	-	-	-	-
	A	.02004	.02045	.01635	-	-	-	-
22	F	.00045	.00825	-	-	-	-	-
	A	.01756	.02092	-	-	-	-	-
23	F	.00047	.00783	-	-	-	-	-
	A	.01813	.01999	-	-	-	-	-
24	F	.00062	.00478	-	-	-	-	-
	A	.02215	.01290	-	-	-	-	-
25	F	.00048	.00837	-	-	-	-	-
	A	.01965	.02319	-	-	-	-	-
26	F	.00041	.00996	-	-	-	-	-
	A	.01724	.02703	-	-	-	-	-

F: Ferrite phase

A: Austenite(Martensite) phase

Table 4.4

Mole fractions of ferrite and martensite in local equilibrium

No. of steps	Phase	C	Mn	Si	Ni	Cr	Mo	Cu
1	F	.00024	.01473	.00008	-	-	-	-
	A	.01006	.01458	.00007	-	-	-	-
2	F	.00021	.01524	.00019	-	-	-	-
	A	.00889	.01511	.00019	-	-	-	-
3	F	.00021	.01526	.00019	-	-	-	-
	A	.00886	.01513	.00019	-	-	-	-
4	F	.00018	.01578	.00019	-	-	-	-
	A	.00766	.01566	.00019	-	-	-	-
5a	F	.00004	.01531	.00476	-	-	-	-
	A	.00130	.01529	.00475	-	-	-	-
b	F	.00010	.01530	.00475	-	-	-	-
	A	.00350	.01525	.00473	-	-	-	-
c	F	.00016	.01530	.00475	-	-	-	-
	A	.00624	.01521	.00473	-	-	-	-
6a	F	.00006	.01491	.00456	-	-	-	-
	A	.00182	.01488	.00455	-	-	-	-
b	F	.00012	.01491	.00456	-	-	-	-
	A	.00413	.01485	.00454	-	-	-	-
c	F	.00018	.01491	.00456	-	-	-	-
	A	.00699	.01481	.00453	-	-	-	-
7a	F	.00006	.01492	.00476	-	-	-	-
	A	.00183	.01489	5.00475	-	-	-	-
b	F	.00012	.01492	.00476	-	-	-	-
	A	.00412	.01486	.00474	-	-	-	-
c	F	.00018	.01491	.00476	-	-	-	-
	A	.00696	.01481	.00495	-	-	-	-
8a	F	.00003	.01553	.00476	-	-	-	-
	A	.00099	.01552	.00476	-	-	-	-

Table 4.4 continued

b	F	.00009	.01553	.00476	-	-	-	-
	A	.00314	.01548	.00475	-	-	-	-
c	F	.00015	.01553	.00476	-	-	-	-
	A	.00581	.01544	.00474	-	-	-	-
9a	F	.00003	.01554	.00496	-	-	-	-
	A	.00100	.01552	.00496	-	-	-	-
b	F	.00009	.01554	.00496	-	-	-	-
	A	.00314	.01549	.00495	-	-	-	-
c	F	.00015	.01553	.00496	-	-	-	-
	A	.00579	.01545	.00493	-	-	-	-
10a	F	.00004	.01535	.00457	-	-	-	-
	A	.00122	.01533	.00457	-	-	-	-
b	F	.00010	.01535	.00457	-	-	-	-
	A	.00343	.01530	.00455	-	-	-	-
c	F	.00016	.01535	.00457	-	-	-	-
	A	.00617	.01526	.00454	-	-	-	-
11	F	.00056	.00507	.00595	-	-	-	-
	A	.02596	.00494	.00579	-	-	-	-
12	F	.00016	.01516	.01285	-	-	-	-
	A	.00672	.01506	.01276	-	-	-	-
13a	F	.00025	.01425	-	-	-	-	-
	A	.01027	.01411	-	-	-	-	-
b	F	.00027	.01425	-	-	-	-	-
	A	.01195	.01408	-	-	-	-	-
c	F	.00029	.01425	-	-	-	-	-
	A	.01351	.01406	-	-	-	-	-
d	F	.00030	.01425	-	-	-	-	-
	A	.01491	.01404	-	-	-	-	-
e	F	.00015	.01425	-	-	-	-	-
	A	.00512	.01418	-	-	-	-	-
f	F	.00022	.01425	-	-	-	-	-
	A	.00851	.01413	-	-	-	-	-
14a	F	.00057	.00325	-	-	-	-	-
	A	.02067	.00318	-	-	-	-	-

Table 4.4 continued

d	F	.00060	.00325	-	-	-	-	-
	A	.02344	.00317	-	-	-	-	-
e	F	.00063	.00325	-	-	-	-	-
	A	.02642	.00316	-	-	-	-	-
f	F	.00066	.00325	-	-	-	-	-
	A	.02956	.00315	-	-	-	-	-
g	F	.00068	.00325	-	-	-	-	-
	A	.03279	.00314	-	-	-	-	-
h	F	.00069	.00325	-	-	-	-	-
	A	.03612	.00313	-	-	-	-	-
i	F	.00070	.00325	-	-	-	-	-
	A	.03953	.00312	-	-	-	-	-
15a	F	.00055	.00386	-	-	-	-	-
	A	.01992	.00278	-	-	-	-	-
b	F	.00058	.00386	-	-	-	-	-
	A	.02264	.00377	-	-	-	-	-
c	F	.00061	.00386	-	-	-	-	-
	A	.02556	.00376	-	-	-	-	-
d	F	.00064	.00386	-	-	-	-	-
	A	.02865	.00375	-	-	-	-	-
e'	F	.00066	.00386	-	-	-	-	-
	A	.03181	.00374	-	-	-	-	-
f	F	.00067	.00386	-	-	-	-	-
	A	.03506	.00373	-	-	-	-	-
g	F	.00068	.00386	-	-	-	-	-
	A	.03838	.00371	-	-	-	-	-
16	F	.00037	.01016	-	-	-	-	-
	A	.01361	.01003	-	-	-	-	-
17	F	.00014	.01524	-	-	-	-	-
	A	.00496	.01517	-	-	-	-	-
18	F	.00037	.01016	-	-	-	-	-
	A	.01362	.01002	-	-	-	-	-
19	F	.00049	-	-	.00952	-	-	-
	A	.02026	-	-	.00933	-	-	-

Table 4.4 continued

20	F	-	-	-	-	-	-	-
	A	-	-	-	-	-	-	-
21	F	.00022	.01007	.01969	-	-	-	-
	A	.00843	.00998	.01953	-	-	-	-
22	F	.00038	.00986	-	-	-	-	-
	A	.01409	.00972	-	-	-	-	-
23	F	.00037	.01006	-	-	-	-	-
	A	.01377	.00993	-	-	-	-	-
24	F	.00038	.00988	-	-	-	-	-
	A	.01405	.00975	-	-	-	-	-
25	F	.00017	.01527	-	-	-	-	-
	A	.00650	.01517	-	-	-	-	-
26	F	.00017	.01526	-	-	-	-	-
	A	.00652	.01516	-	-	-	-	-

F: Ferrite phase

A: Austenite(Martensite) phase

Table 5.1

Salt bath composition (45)

Operating temperature range (Degs K)	$BaCl_2$	NaCl	KCl
815-1100	85-95%	5-15%	-
590-900	50-60%	15-25%	20-32%

Table 5.1a

Measured volume fractions of martensite (intermediate quenching)

Temp	volume fraction of martensite at different holding times(Secs)					Vm
(Deg K)	5	60	120	300	600	calculated
1033	.233	.405	.517	.531	.554	.627499
1013	.164	.353	.427	.434	.456	.474045
993	.046	.214	.251	.273	.290	.368617

Table 5.2b

Measured volume fractions of martensite (intermediate normalising)

Temp	volume fraction of martensite at different holding times(Secs)					Vm
(Deg K)	5	60	120	300	600	calculated
1033	.226	.432	.484	.527	.549	.627499
1013	.156	.334	.391	.403	.438	.474045
993	.067	.216	.273	.296	.315	.368617

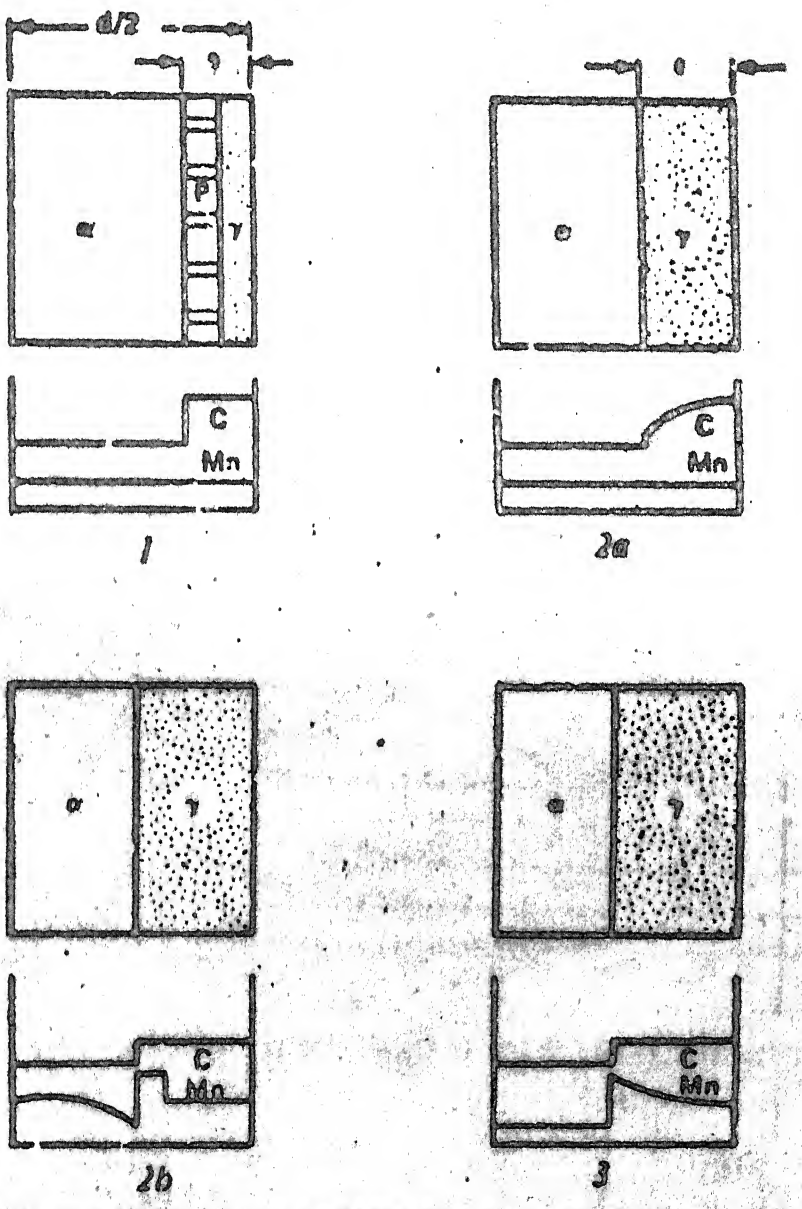

CENTRAL LIBRARY
I. I. T., Kanpur
Acc. No. A 82544

Fig. 2.1 –Schematic diagrams of three steps in austenite growth during intercritical annealing of ferrite-pearlite steels. (1) Dissolution of pearlite; (2a) Austenite growth with carbon diffusion in austenite; (2b) Austenite growth with manganese diffusion in ferrite; and (3) Final equilibration with manganese diffusion in austenite.

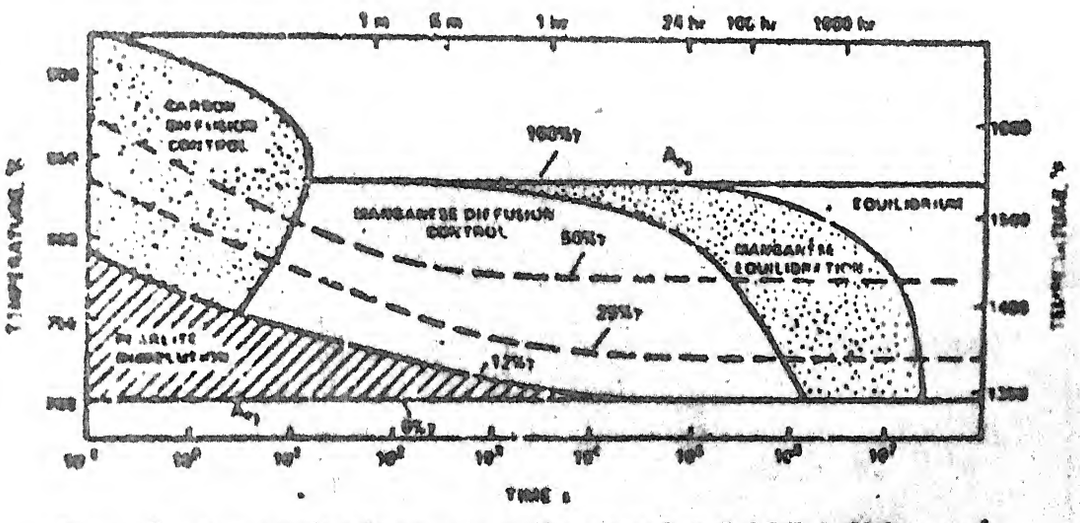

Fig.2.2—Austenite formation diagram for 0.12C-1.5Mn steel.

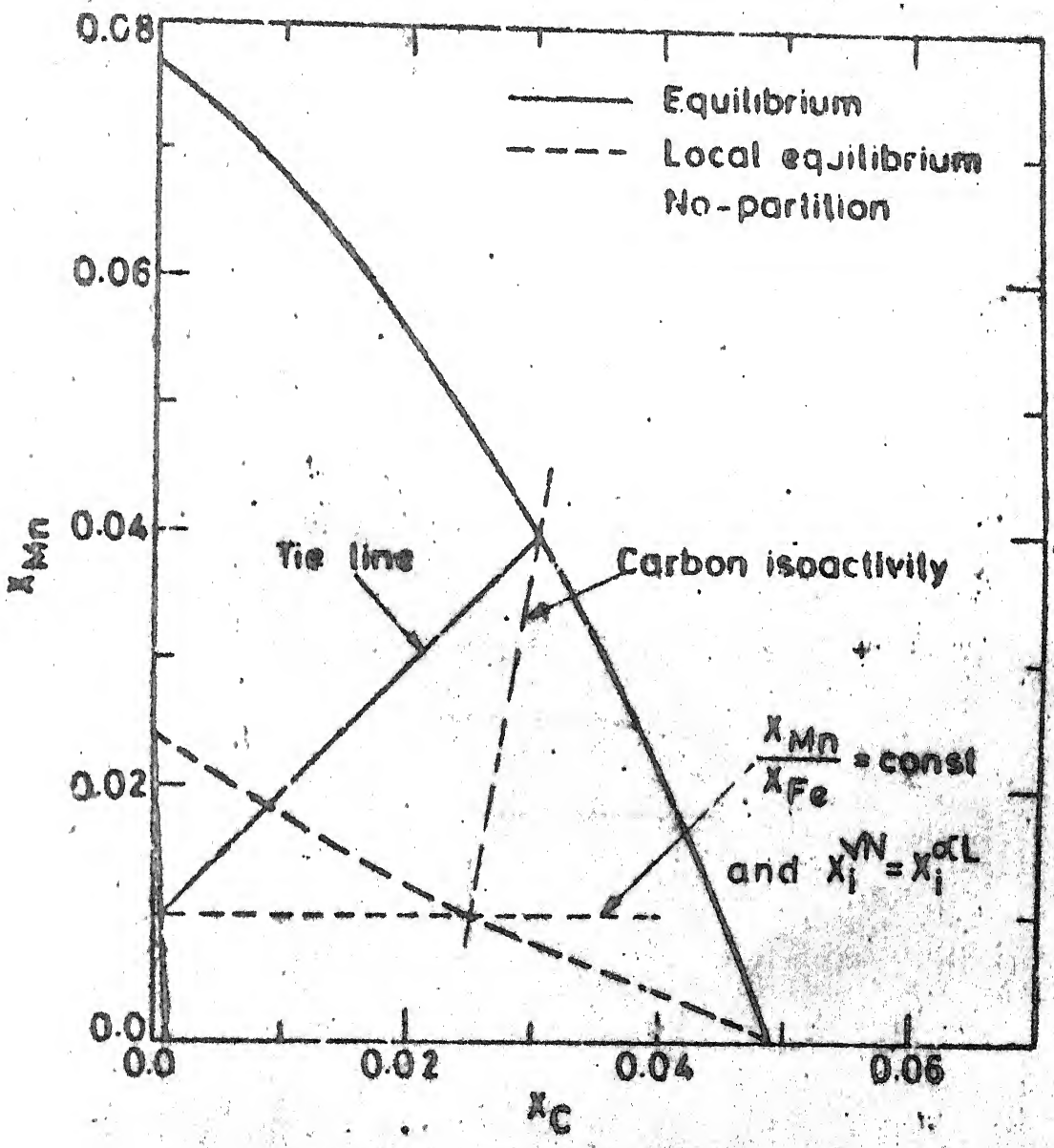

Fig. 2.3 Equilibrium and local equilibrium No-partition boundaries at 960K.

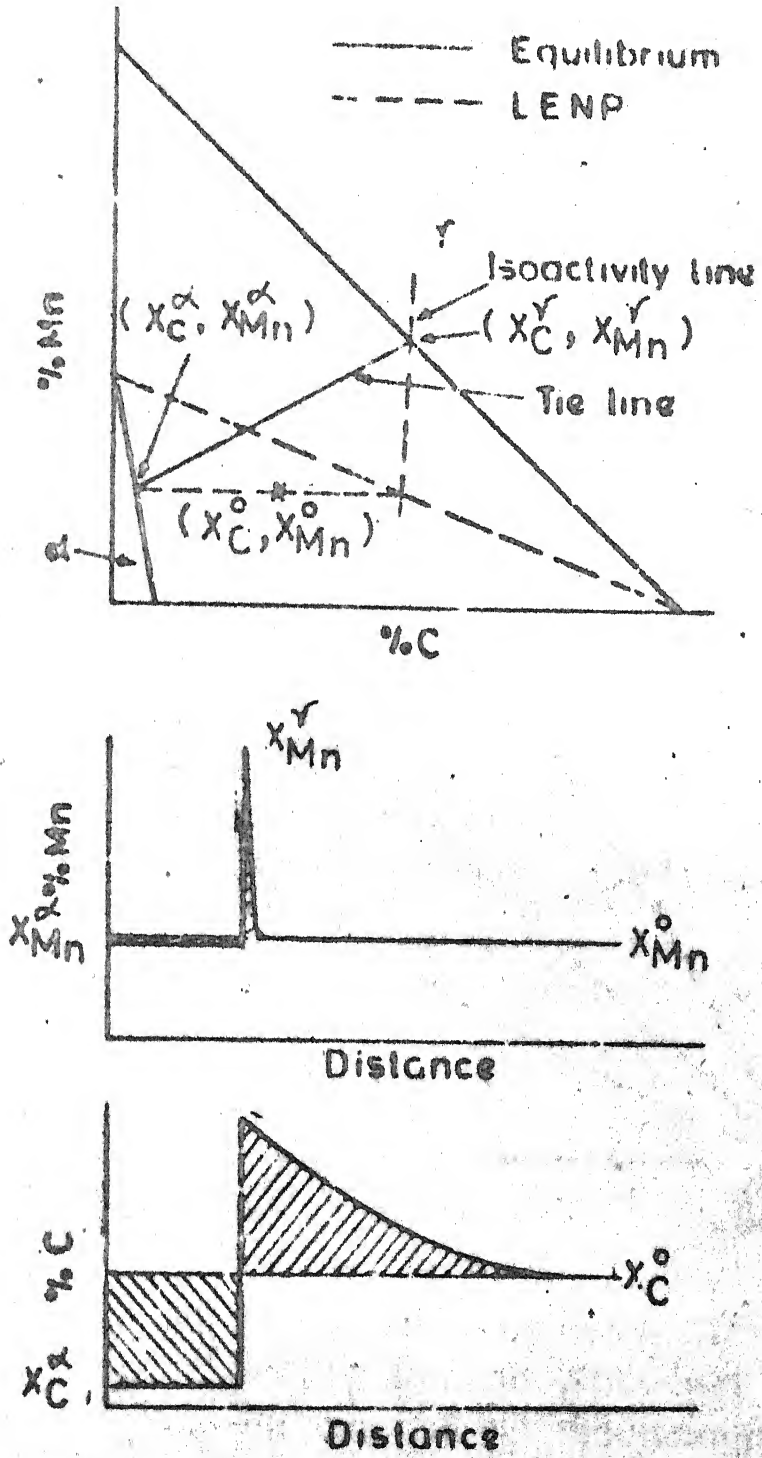

Fig. 2.4 Schematic penetration curves for carbon and manganese during the ferrite growth by LENP mechanism.

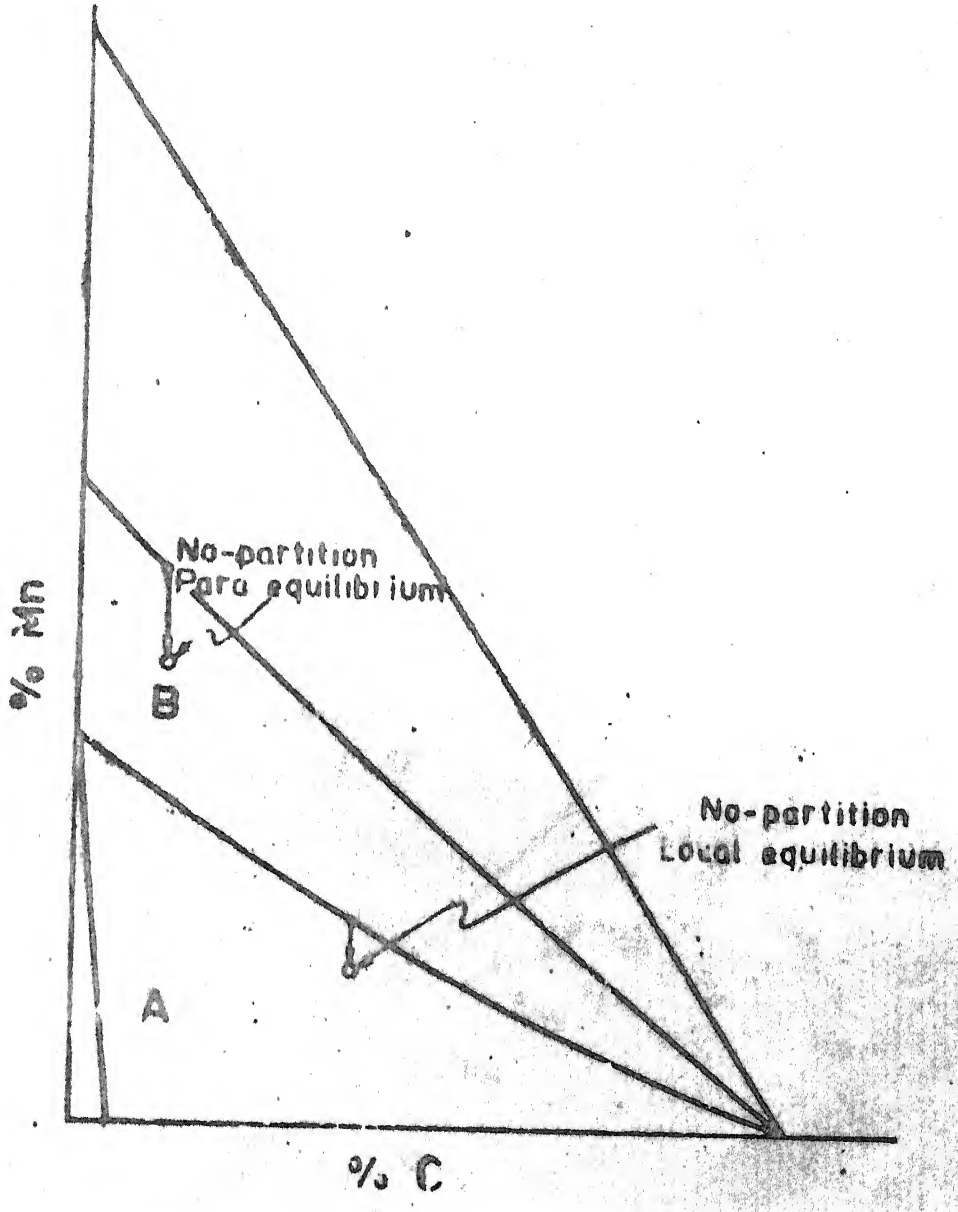

Fig.25 Schematic representation of regions where the no-partition reactions by PE and LENP mechanisms is feasible.

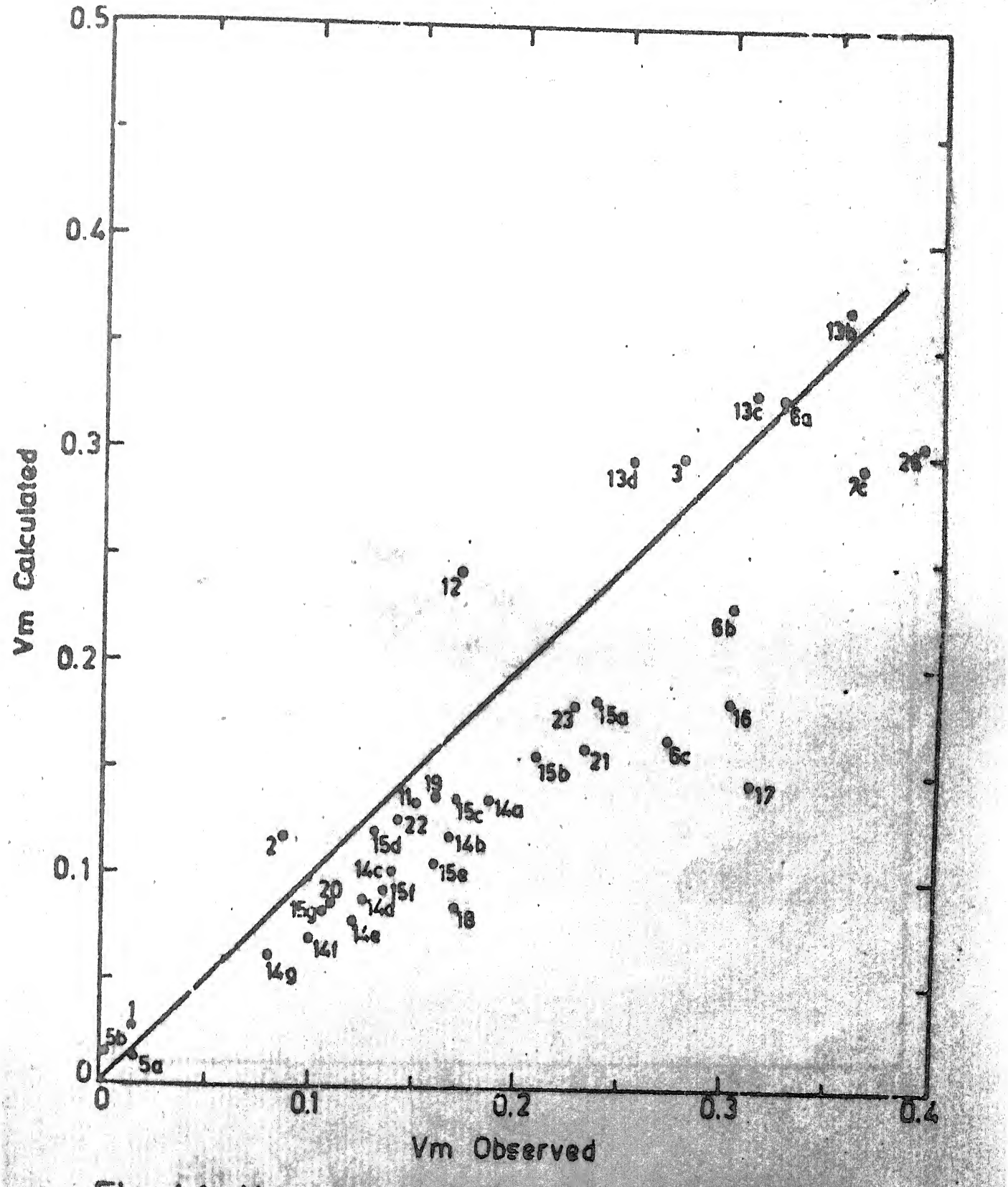

Fig. 4.1. Vm observed Vs Vm calculated.

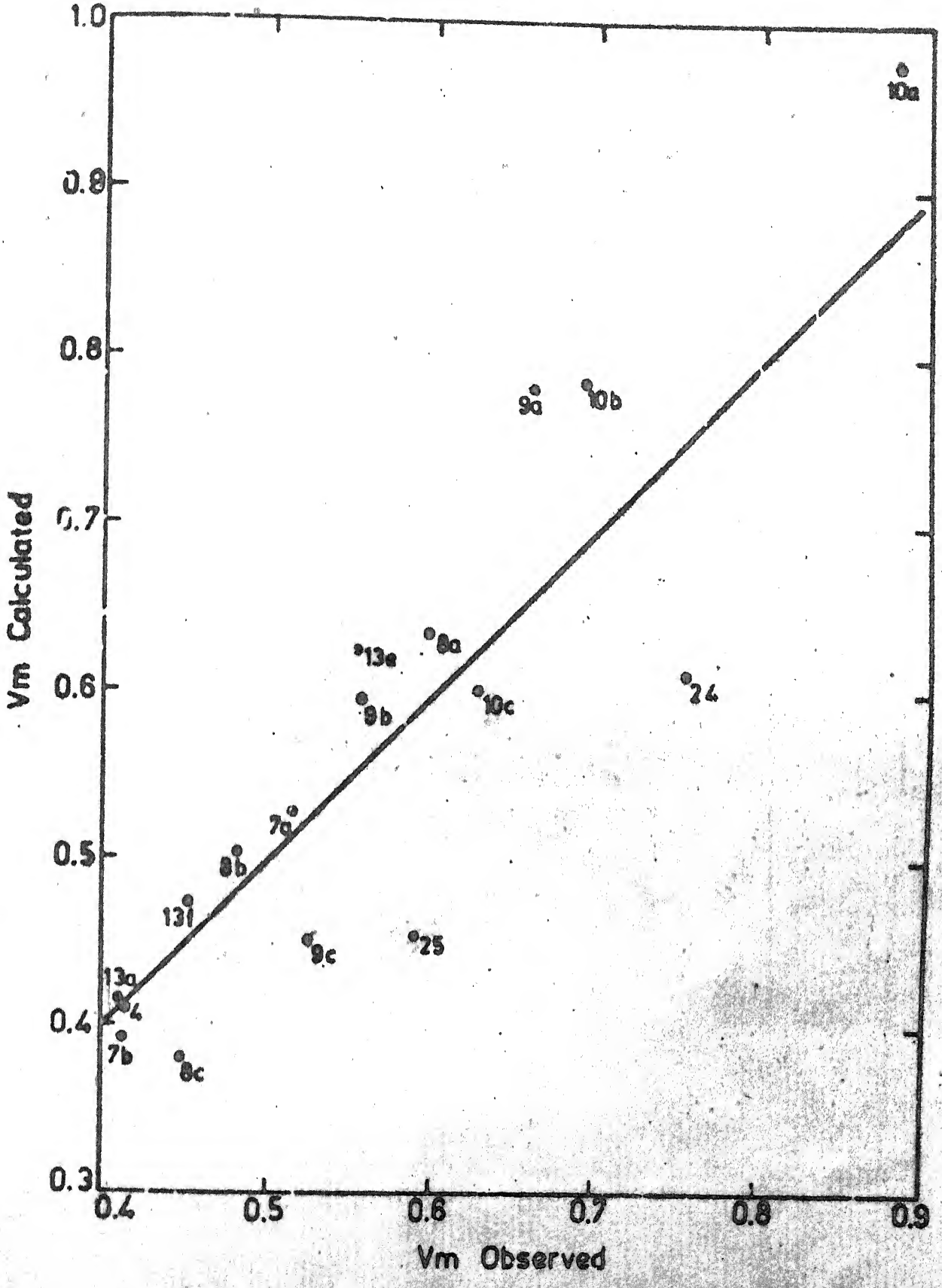

Fig. 4.2. Vm observed Vs Vm calculated.

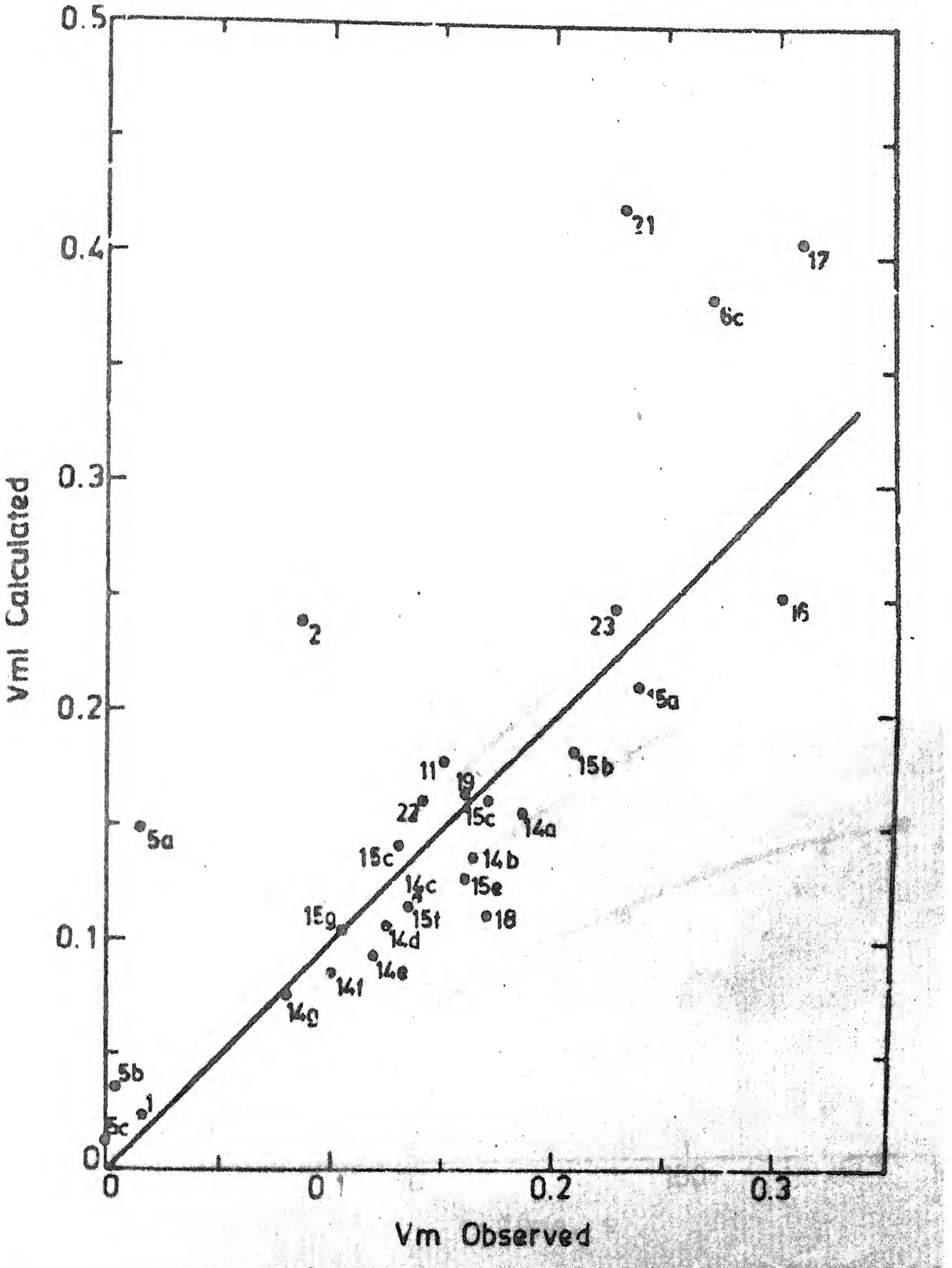

Fig. 4.3 Vm served Vs Vml calculated.

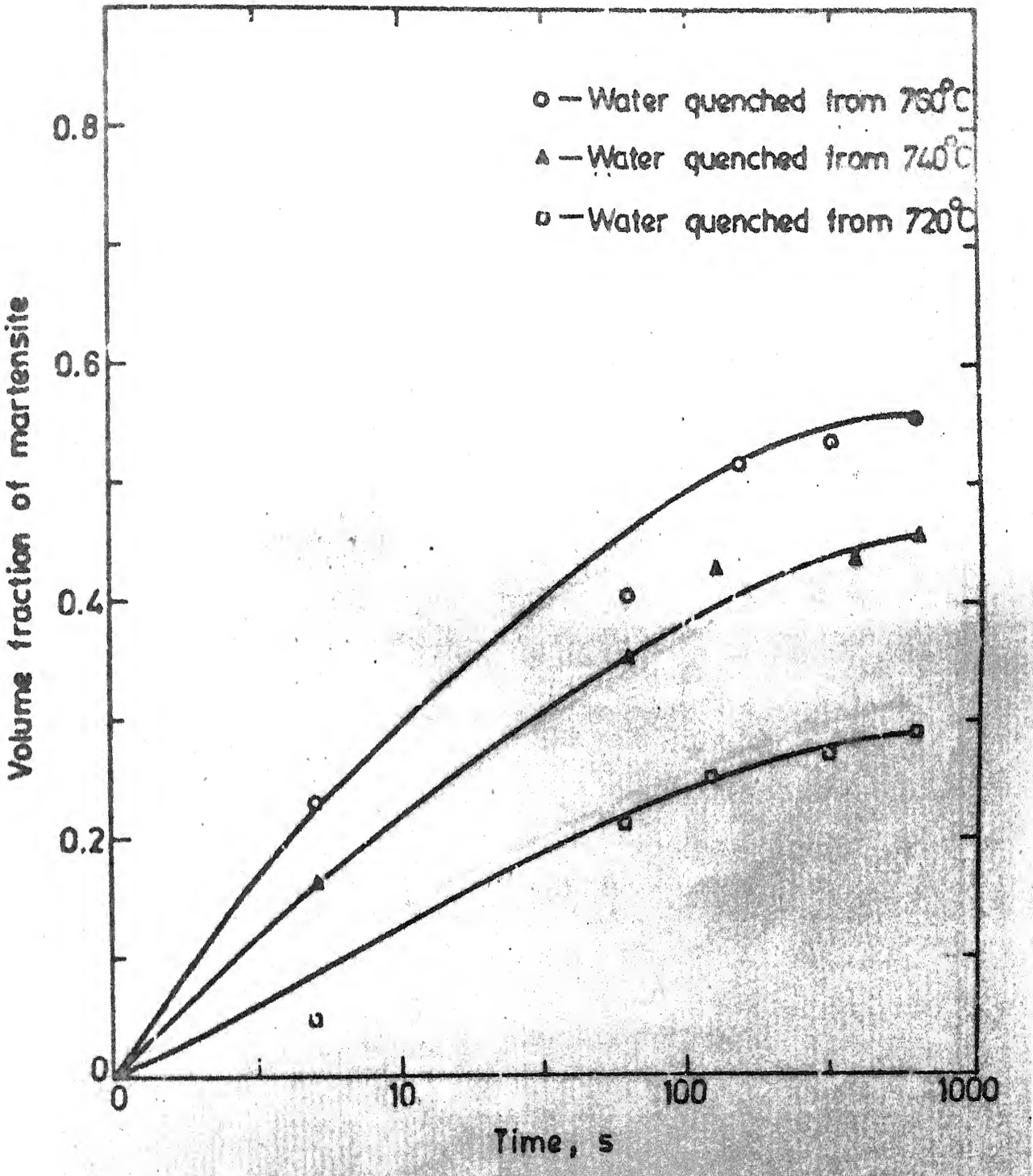

Fig. 5.1. Formation of martensite in 0.22 C - 1.4 Mn steel during intermediate quenching.

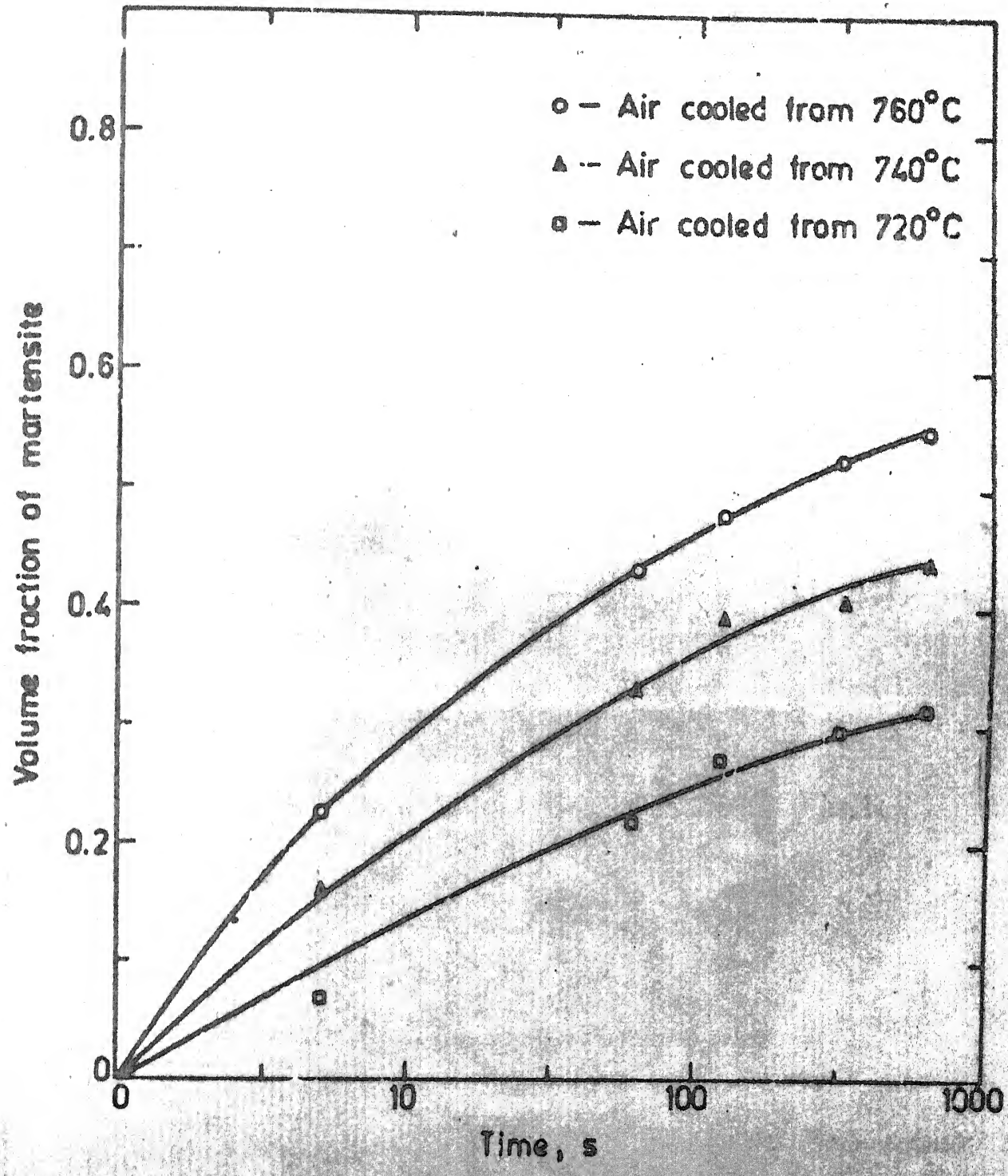

Fig. 5.2. Formation of martensite in 0.22 C - 1.4 Mn steel during intermediate normalising.

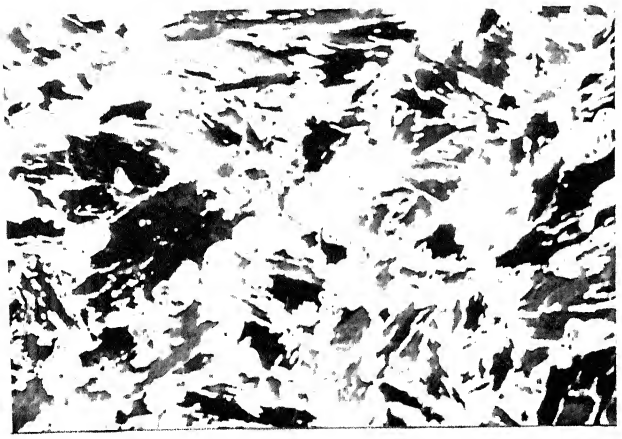

(a)

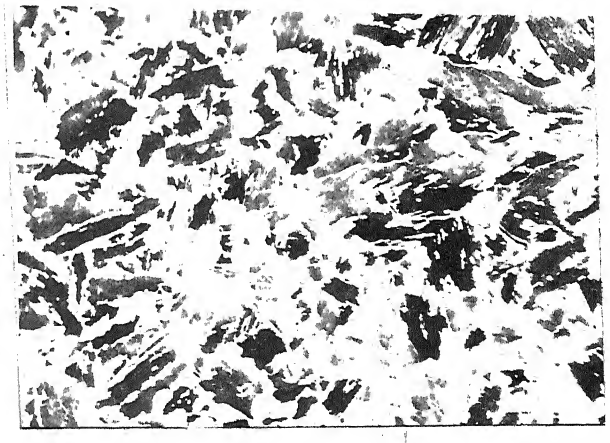

(b)

(c)

(d)

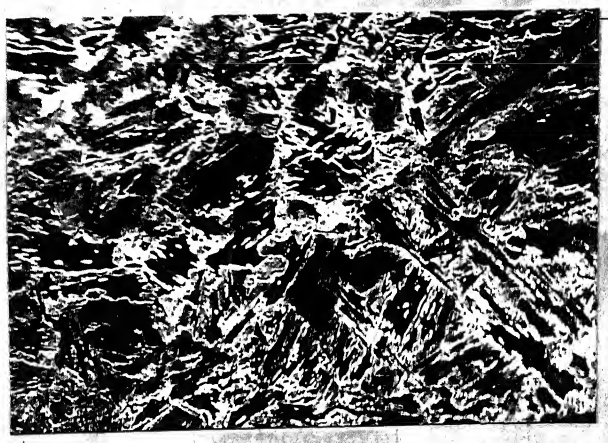

(e)

Figure 5.3 Micrographs of 0.22 C-1.4 Mn steel intercritically annealed at 720°C for (a) 5 s, (b) 1 m, (c) 2 m, (d) 5 m and (e) 10 m.

EXPLANATION OF THE SYMBOLS EMPLOYED

AC : The activity of carbon

DSGFT: The tabulated values of the change in free energy

DENMX: The common denominator of the mole fraction computations

DGI : The free energy values of the element I (I=C, Mn ,Si, Ni, Cr, Mo, Cu, Fe)

DA1 : The denominator used in computation of elemental percentages in austenite

DA2 : The denominator used in computation of elemental percentages in ferrite

EATI : The self interaction parameter of the element I in the austenite

EFII : The self interaction parameter of element I in ferrite

EII : The cross interaction parameter between element I and carbon in both austenite and ferrite

FUNN : The function (T) (in Equation (3.24))

FUNA : The value of FUNN in temperature T

FUNB : The value of FUNN in temperature T+H

FO : The value of FO (in Equation (3.21))

FI : The value of FI for I= C,MN,SI,NI,CR,MO,CU (in Equations (3.22) and (3.23))

G(I) : The activity coefficient of element I in austenite and ferrite denoted as gamma(i) in equation (3.13)

H : The temperature increment in the Ae3 subprogramme

I,IL,IK,J,JT,JUY,JG,JYT,JK,JU: Dummy scripts

PI : The original percentage of alloying element in the steel

PAI : The percentage of alloying element I in austenite in complete equilibrium condition

PFI : The percentage of element I in ferrite in complete equilibrium condition

PLI : The percentage of element I in austenite in local equilibrium no partioning conditon

PLI : The percentage of element I in ferrite in local equilibrium no partioning conditon

PNI : The percentage of element I in austenite for iso activity of carbon

T : The temperature at which the steel has been heat treated

TAEN : The Ae3 temperature in degree K

TEMP : The temperature corresponding to DSGFE

VALPHA: The volume fraction of ferrite in complete equilibrium

VLALPH: The volume fraction of ferrite in local equilibrium

VMTNST: The volume fraction of martensite phase in complete equilibrium

VLMNST: The volume fraction of martensite in local equilibrium

WKSPCE: The work space

XI : The mole fraction of element I in the steel originally

X(I) : The mole fraction of element I in austenite for I=1,7

Y(I) : The mole fraction of element I in ferrite for I=8,14

XL(I): The mole fraction of element I in austenite and ferrite in local equilibrium no partitioning condition

XNI : The mole fraction of element I in austenite for iso activity of carbon

ZA,ZB,ZC: Substitutes for mole fractions in subroutine

APPENDIX I

```
C*****************************************************************
C     * PROGRAM FOR COMPUTATION OF ELEMENTAL COMPOSITION OF DUAL
C       PHASE STEELS IN FERRITE AND AUSTENITE SEPERATELY *
C*****************************************************************
      DIMENSION TEMP(57),DSGFE(57),X(15),XN(7),XL(14),G(16)
      DIMENSION ZA(14,14),ZB(14,1),ZC(14,1),WKSPCE(200)
      OPEN(UNIT=22,FILE='COM.DAT')
      DO 100 K=1,57
      READ*,TEMP(K),DSGFE(K)
  100 CONTINUE
      NS=1
      DO 101 G=1,NS
      READ*,PC,PMN,PSI,PNI,PCR,PMO,PCU
      G=0.0001
C*****************************************************************
C                  * MOLE FRACTION CALCULATIONS *
C*****************************************************************
      WRITE(22,103)
  103 FORMAT(////16X,'COMPUTATION OF MOLE FRACTIONS OF STEEL IN FERRIT
     1E AND AUSTENITE'/ )
      WRITE(22,104)
  104 FORMAT(16X,1HO,8X,'* COMPOSITION OF STEEL IN WEIGHT PERCENTAGE *
     1'/)
      WRITE(22,108)
  108 FORMAT(16X,1HO,3X,'C',6X,'Mn',7X,'Si',6X,'Ni',5X,'Cr',6X,'Mo',6X
     1,'Cu',4X,'Temp')
      WRITE(22,105)PC,PMN,PSI,PNI,PCR,PMO,PCU,T
  105 FORMAT(16X,1HO,7(F6.4,2X),F6.1/)
      WRITE(22,107)
  107 FORMAT(16X,1HO,4X,'XC',6X,'XMn',6X,'XSi',6X,'XNi',6X,'XCr',6X,
     1'XMO',6X,'XCu')
      DENMX=(100.0-PC-PMN-PSI-PNI-PCR-PMO-PCU)/55.847+PC/12.011
     1+PMN/54.938+PSI/28.086+PNI/58.71+PCR/51.996+PMO/95.94+PCU/63.54
      IF(PC.EQ.0.0) GO TO 110
      XC=(PC/12.011)/DENMX
      GO TO 111
  110 XC=10.0E-9
  111 IF(PMN.EQ.0.0) GO TO 112
      XMN=(PMN/54.938)/DENMX
      GO TO 113
  112 XMN=10.0E-9
  113 IF(PSI.EQ.0.0) GO TO 114
      XSI=(PSI/28.086)/DENMX
      GO TO 115
  114 XSI=10.0E-9
  115 IF(PNI.EQ.0.0) GO TO 116
      XNI=(PNI/58.71)/DENMX
      GO TO 117
  116 XNI=10.0E-9
  117 IF(PCR.EQ.0.0) GO TO 118
      XCR=(PCR/51.996)/DENMX
      GO TO 119
  118 XCR=10.0E-9
  119 IF(PMO.EQ.0.0) GO TO 120
      XMO=(PMO/95.94)/DENMX
      GO TO 121
  120 XMO=10.0E-9
  121 IF(PCU.EQ.0.0) GO TO 122
      XCU=(PCU/63.54)/DENMX
      GO TO 123
  122 XCU=10.0E-9
  123 WRITE(22,124)XC,XMN,XSI,XNI,XCR,XMO,XCU
  124 FORMAT(16X,1HO,7(F8.6,1X)/)
      T=F
```

```
      I=I+1
      IF(I-IEMP(I)) 126,126,125
      DOGFE=DSGFE(I-1)+(DSGFE(J)-DSGFE(J-1))*(T-TEMP(J-1))/(TEMP(J)
     1-TEMP(J-1))

C*****************************************************************

C             * INTERACTION PARAMETER CALCULATIONS *

C*****************************************************************

      EA11=8910.0/T
      E21=-4950.0/T
      EA22=220.0/T
      E31=12650.0/T
      EA33=(-3059.0/T)-41.0377+9.9873*ALOG(T)
      E41=5170.0/T
      EA44=-1870.0/T
      E51=-14080.0/T
      EA55=330.0/T
      E61=-10670.0/T
      EA66=-2310.0/T
      E71=4180.0/T
      EA77=-7260.0/T
      EF11=0.0
      EF22=-990.0/T
      EF33=(-21787.0/T)+6.4544+5.2320*ALOG(T)
      EF44=-1870.0/T
      EF55=-2970.0/T
      EF66=-4290.0/T
      EF77=-8910.0/T

C*****************************************************************

C             * CALCULATION OF CHANGE IN FREE ENERGY *

C*****************************************************************

      DOGC=7.6866*T-15323.0
      DOGMN=-38795.0+62.137*T-0.0255*((T)**2)
      DOGSI=-5964.0+38.7996*T-4.7244*T*ALOG(T)
      DOGNI=3.233*T-4545.0
      DOGCR=-367.0-4.656*T+0.6568*T*ALOG(T)
      DOGMO=565.0+0.15*T
      DOGCU=-0.017*((T)**2)+41.183*T-25500.0

C*****************************************************************

C  * COMPOSITION CALCULATIONS IN COMPLETE EQUILIBRIUM CONDITION *

C*****************************************************************

      X(1)=XC
      X(2)=XMN
      X(3)=XSI
      X(4)=XNI
      X(5)=XCR
      X(6)=XMO
      X(7)=XCU
      X(8)=XC*EXP(DOGC/(1.987*T))
      X(9)=XMN*EXP(DOGMN/(1.987*T))
      X(10)=XSI*EXP(DOGSI/(1.987*T))
      X(11)=XNI*EXP(DOGNI/(1.987*T))
      X(12)=XCR*EXP(DOGCR/(1.987*T))
      X(13)=XMO*EXP(DOGMO/(1.987*T))
      X(14)=XCU*EXP(DOGCU/(1.987*T))
      DO 130 I=1,15
      XOLD=X(I)
      F0=-DOGFE/(1.987*T)
     1-X(8)*(E21*X(9)+E31*X(10)+E41*X(11)+E51*X(12)+E61*X(13)+E71*
     1X(14))-(EF11*X(8)**2+EF22*X(9)**2+EF33*X(10)**2+EF44*X(11)**2+
     1EF55*X(12)**2+EF66*X(13)**2+EF77*X(14)**2)/2.0
```

```
F1=DOGC/(1.987*T)+EA11*X(1)+F21*X(2)+E31*X(3)+E41*X(4)+E51*X(5)
1+E61*X(6)+E71*X(7)
F2=DOGMN/(1.987*T)+E21*X(1)+EA22*X(2)
F3=DOGSI/(1.987*T)+E31*X(1)+EA33*X(3)
F4=DOGNI/(1.987*T)+E41*X(1)+EA44*X(4)
F5=DOGCR/(1.987*T)+E51*X(1)+EA55*X(5)
F6=DOGMO/(1.987*T)+E61*X(1)+EA66*X(6)
F7=DOGCU/(1.987*T)+E71*X(1)+EA77*X(7)
X(1)=(1-X(1)-X(2)-X(3)-X(4)-X(5)-X(6)-X(7))-(1-X(8)-X(9)-X(10)
1-X(11)-X(12)-X(13)-X(14))*EXP(F0+X1*(E21*X(2)+E31*X(3)+E41*X(4)
1+E51*X(5)+E61*X(6)+E71*X(7))+(EA11*X(1)**2+EA22*X(2)**2+EA33*
1X(3)**2+EA44*X(4)**2+EA55*X(5)**2+EA66*X(6)**2+EA77*X(7)**2)/2)
X(2)=(XMN-X(9)*X(15))/(1-X(15))
X(3)=(XSI-X(10)*X(15))/(1.-X(15))
X(4)=(XNI-X(11)*X(15))/(1.-X(15))
X(5)=(XCR-X(12)*X(15))/(1.-X(15))
X(6)=(XMO-X(13)*X(15))/(1.-X(15))
X(7)=(XCU-X(14)*X(15))/(1.-X(15))
X(8)=X(1)*EXP(F1-EF11*X(8)-E21*X(9)-E31*X(10)-E41*X(11)-E51*
1X(12)+E61*X(13)+E71*X(14))
X(9)=X(2)*EXP(F2-EF22*X(9)-E21*X(8))
X(101)=X(3)*EXP(F3-EF33*X(10)-E31*X(8))
X(102)=X(3)*EXP(F3-EF33*X(101)-E31*X(8))
X(103)=X(3)*EXP(F3-EF33*X(102)-E31*X(8))
IF(ABS(X(103)-2.0*X(102)+X(101)).LT.0.000001) GO TO 148
A=(X(103)-X(102))/(X(103)-2.0*X(102)+X(101))
X(10)=A*X(102)+(1.0-A)*X(103)
GO TO 149
X(10)=X(103)
X(11)=X(4)*EXP(F4-EF44*X(11)-E41*X(8))
X(12)=X(5)*EXP(F5-EF55*X(12)-E51*X(8))
X(13)=X(6)*EXP(F6-EF66*X(13)-E61*X(8))
X(14)=X(7)*EXP(F7-EF77*X(14)-E71*X(8))
X(15)=(XC-X(1))/(X(8)-X(1))
XNEW=X(1)
IF(ABS(XOLD-XNEW)<=0.000001) GO TO 135
GO TO 129
CONTINUE

*****************************************************************

   * COMPOSITION CALCULATION IN LOCAL EQUILIBRIUM CONDITION *

*****************************************************************

XL(1)=XC*EXP(DOGC/(1.987*T))
XL(2)=XMN*EXP(-DOGMN/(1.987*T))
XL(3)=XSI*EXP(-DOGSI/(1.987*T))
XL(4)=XNI*EXP(-DOGNI/(1.987*T))
XL(5)=XCR*EXP(-DOGCR/(1.987*T))
XL(6)=XMO*EXP(-DOGMO/(1.987*T))
XL(7)=XCU*EXP(-DOGCU/(1.987*T))
XL(8)=X(8)
XL(9)=XMN
XL(10)=XSI
XL(11)=XNI
XL(12)=XCR
XL(13)=XMO
XL(14)=XCU
XFE=(1-XC-XMN-XSI-XNI-XCR-XMO-XCU)
DO 192 I=1,14
XLOLD=XL(I)
FL0=-DOGFE/(1.987*T)
1-XL(1)*(E21*XL(2)+E31*XL(3)+E41*XL(4)+E51*XL(5)+E61*XL(6)+
1E71*XL(7))-(EF11*XL(8)**2+EF22*XL(9)**2+EF33*XL(10)**2+EF44*
1XL(11)**2+EF55*XL(12)**2+EF66*XL(13)**2+EF77*XL(14)**2)/2.0
FL1=DOGC/(1.987*T)+(EF11*XL(8)+E21*XL(9)+E31*XL(10)+E41*XL(11)+
1E51*XL(12)+E61*XL(13)+E71*XL(14))
FL2=-DOGMN/(1.987*T)-(E21*XL(8)+EF22*XL(9))
FL3=-DOGSI/(1.987*T)-(E31*XL(8)+EF33*XL(10))
FL4=-DOGNI/(1.987*T)-(E41*XL(8)+EF44*XL(11))
FL5=-DOGCR/(1.987*T)-(E51*XL(8)+EF55*XL(12))
FL6=-DOGMO/(1.987*T)-(E61*XL(8)+EF66*XL(13))
FL7=-DOGCU/(1.987*T)-(E71*XL(8)+EF77*XL(14))
XL(1)=(1-XL(2)-XL(3)-XL(4)-XL(5)-XL(6)-XL(7))-(1-XL(9)-XL(9)-
1XL(10)-XL(11)-XL(12)-XL(13)-XL(14))*EXP(FL0+XL(1)*(E21*XL(2)+
```

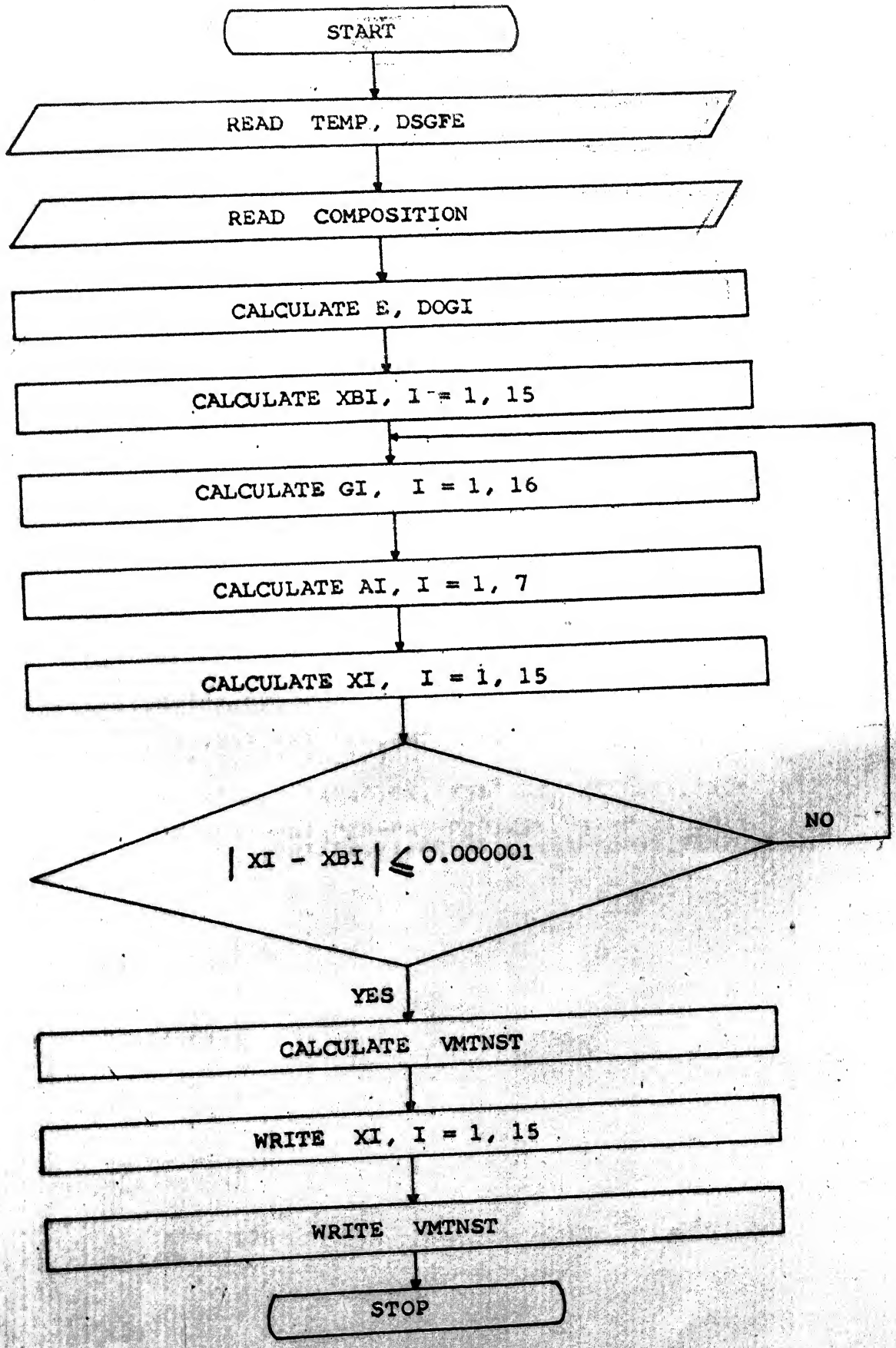

The flow chart for the calculation of the martensite volume fraction in complete equilibrium condition.

Appendix II

```
************************************************************************
    * PROGRAM FOR COMPUTATION OF ELEMENTAL COMPOSITION OF DUAL
        PHASE STEELS IN FERRITE AND AUSTENITE SEPERATELY *
************************************************************************

      DIMENSION TEMP(57),DSGFE(57),X(15),XN(7),XL(14),XB(14),G(16)
      DIMENSION ZA(14,14),ZB(14,1),ZC(14,1),WKSPCE(200)
      OPEN(UNIT=22,FILE='COM.DAT')
      DO 100 K=1,57
      READ*,TEMP(K),DSGFE(K)
  100 CONTINUE
      NS=1
      DO 101 L=1,NS
      READ*,PC,PMN,PSI,PNI,PCR,PMO,PCU,T
************************************************************************
                    * MOLE FRACTION CALCULATIONS *
************************************************************************

      WRITE(22,103)
  103 FORMAT(///16X,'COMPUTATION OF MOLE FRACTIONS OF STEEL IN FERRIT
     1E AND AUSTENITE'/ )
      WRITE(22,104)
  104 FORMAT(16X,1HO,8X,'* COMPOSITION OF STEEL IN WEIGHT PERCENTAGE *
     1'/)
      WRITE(22,108)
  108 FORMAT(16X,1HO,3X,'C',6X,'Mn',7X,'Si',6X,'Ni',6X,'Cr',6X,'Mo',6X
     1,'Cu',4X,'Temp')
      WRITE(22,105)PC,PMN,PSI,PNI,PCR,PMO,PCU,T
  105 FORMAT(16X,1HO,7(F6.4,2X),F6.1/)
      WRITE(22,107)
  107 FORMAT(16X,1HO,4X,'XC',6X,'XMN',6X,'XSI',6X,'XNI',6X,'XCr',6X,
     1'XMO',6X,'XCu')
      DENMX=(100.0-PC-PMN-PSI-PNI-PCR-PMO-PCU)/55.847+PC/12.011
     1+PMN/54.938+PSI/28.086+PNI/58.71+PCR/51.996+PMO/95.94+PCU/63.54
      IF(PC.EQ.0.0) GO TO 110
      XC=(PC/12.011)/DENMX
      GO TO 111
  110 XC=10.0E-9
  111 IF(PMN.EQ.0.0) GO TO 112
      XMN=(PMN/54.938)/DENMX
      GO TO 113
  112 XMN=10.0E-9
  113 IF(PSI.EQ.0.0) GO TO 114
      XSI=(PSI/28.086)/DENMX
      GO TO 115
  114 XSI=10.0E-9
  115 IF(PNI.EQ.0.0) GO TO 116
      XNI=(PNI/58.71)/DENMX
      GO TO 117
  116 XNI=10.0E-9
  117 IF(PCR.EQ.0.0) GO TO 118
      XCR=(PCR/51.996)/DENMX
      GO TO 119
  118 XCR=10.0E-9
  119 IF(PMO.EQ.0.0) GO TO 120
      XMO=(PMO/95.94)/DENMX
      GO TO 121
  120 XMO=10.0E-9
  121 IF(PCU.EQ.0.0) GO TO 122
      XCU=(PCU/63.54)/DENMX
      GO TO 123
  122 XCU=10.0E-9
  123 WRITE(22,124)XC,XMN,XSI,XNI,XCR,XMO,XCU
  124 FORMAT(16X,1HO,7(F8.6,1X)/)
      I=K
      T=1
      T=T+1
      IF(1-TEMP(J)) 126,126,125
```

```
DOGFE=DSGFE(J-1)+(DSGFE(J)-DSGFE(J-1))*(T-TEMP(J-1))/(TEMP(J)
1-TEMP(J-1))

*****************************************************************

            * INTERACTION PARAMETER CALCULATIONS *

*****************************************************************

EA11=8910.0/T
E21=-4950.0/T
EA22=220.0/T
E31=12650.0/T
EA33=(-3059.0/T)-41.0377+9.9873*ALOG(T)
E41=5170.0/T
EA44=-1870.0/T
E51=-14080.0/T
EA55=330.0/T
E61=-10670.0/T
EA66=-2310.0/T
E71=4180.0/T
EA77=-7260.0/T
EF11=0.0
EF22=-990.0/T
EF33=(-21787.0/T)+6.4544+5.2320*ALOG(T)
EF44=-1870.0/T
EF55=-2970.0/T
EF66=-4290.0/T
EF77=-8910.0/T

*****************************************************************

          * CALCULATION OF CHANGE IN FREE ENERGY *

*****************************************************************

DOGC=7.6866*T-15323.0
DOGMN=-38795.0+62.137*T-0.0255*((T)**2)
DOGSI=-5964.0+38.7996*T-4.7244*T*ALOG(T)
DOGNI=3.233*T-4545.0
DOGCR=-367.0-4.656*T+0.6568*T*ALOG(T)
DOGMO=565.0+0.15*T
DOGCU=-0.017*((T)**2)+41.183*T-25500.0

*****************************************************************

 * COMPOSITION CALCULATIONS IN COMPLETE EQUILIBRIUM CONDITION *

*****************************************************************

XB(1)=XC
XB(2)=XMN
XB(3)=XSI
XB(4)=XNI
XB(5)=XCR
XB(6)=XMO
XB(7)=XCU
XB(8)=XC*EXP(DOGC/(1.987*T))
XB(9)=XMN*EXP(DOGMN/(1.987*T))
XB(10)=XSI*EXP(DOGSI/(1.987*T))
XB(11)=XNI*EXP(DOGNI/(1.987*T))
XB(12)=XCR*EXP(DOGCR/(1.987*T))
XB(13)=XMO*EXP(DOGMO/(1.987*T))
XB(14)=XCU*EXP(DOGCU/(1.987*T))
X(15)=0.1
G(15)=EXP(-XB(1)*(E21*XB(2)+E31*XB(3)+E41*XB(4)+E51*XB(5)+E61*
1XB(6)+E71*XB(7))-(EA11*XB(1)**2+EA22*XB(2)**2+EA33*XB(3)**2+
1EA44*XB(4)**2+EA55*XB(5)**2+EA66*XB(6)**2+EA77*XB(7)**2)/2.0)
G(16)=EXP(-XB(8)*(E21*XB(9)+E31*XB(10)+E41*XB(11)+E51*XB(12)+E61
1*XB(13)+E71*XB(14))-(EF11*XB(8)**2+EF22*XB(9)**2+EF33*XB(10)**2
1+EF44*XB(11)**2+EF55*XB(12)**2+EF66*XB(13)**2+EF77*XB(14)**2)/
12.0)
G(1)=EXP(EA11*XB(1)+E21*XB(2)+E31*XB(3)+E41*XB(4)+E51*XB(5)+E61*
1XB(6)+E71*XB(7))
G(2)=EXP(E21*XB(1)+EA22*XB(2))
```

```
G(3)=EXP(E31*XB(1)+EA33*XB(3))
G(4)=EXP(E41*XB(1)+EA44*XB(4))
G(5)=EXP(E51*XB(1)+EA55*XB(5))
G(6)=EXP(E61*XB(1)+EA66*XB(6))
G(7)=EXP(E71*XB(1)+EA77*XB(7))
G(8)=EXP(EF11*XB(8)+E21*XB(9)+E31*XB(10)+E41*XB(11)+E51*XB(12)+
1E61*XB(13)+E71*XB(14))
G(9)=EXP(E21*XB(8)+EF22*XB(9))
G(10)=EXP(E31*XB(8)+EF33*XB(10))
G(11)=EXP(E41*XB(8)+EF44*XB(11))
G(12)=EXP(E51*XB(8)+EF55*XB(12))
G(13)=EXP(E61*XB(8)+EF66*XB(13))
G(14)=EXP(E71*XB(8)+EF77*XB(14))
A0=G(15)*EXP(DOGFE/(1.987*T))
A1=G(1)*EXP(DOGC/(1.987*T))
A2=G(2)*EXP(DOGMN/(1.987*T))
A3=G(3)*EXP(DOGSI/(1.987*T))
A4=G(4)*EXP(DOGNI/(1.987*T))
A5=G(5)*EXP(DOGCR/(1.987*T))
A6=G(6)*EXP(DOGMO/(1.987*T))
A7=G(7)*EXP(DOGCU/(1.987*T))
DO 130 I=1,15
XOLD=X(I)
DO 234 I8=1,14;DO  234 J8=1,14;ZA(I8,J8)=0.0
CONTINUE
ZA(1,1)=A1;ZA(1,8)=-G(8);ZA(2,2)=A2;ZA(2,9)=-G(9);ZA(3,3)=A3
ZA(3,10)=-G(10);ZA(4,4)=A4;ZA(4,11)=-G(11);ZA(5,5)=A5
ZA(5,12)=-G(12);ZA(6,6)=A6;ZA(6,13)=-G(13);ZA(7,7)=A7
ZA(7,14)=-G(14);DO 236 JU=1,7;ZA(8,JU)=-A0;JY=7+JU;ZA(8,JY)=G(16)
CONTINUE;JYT=9;DO 237 JK=2,7;JG=JK+7;ZA(JYT,JK)=1.-X(15)
ZA(JYT,JG)=X(15);JYT=JYT+1
CONTINUE
DO  238 JT=1,7;ZB(JT,1)=0.0
CONTINUE;ZB(8,1)=-A0+G(16);ZB(9,1)=XMN;ZB(10,1)=XSI
ZB(11,1)=XNI;ZB(12,1)=XCR;ZB(13,1)=XMO;ZB(14,1)=XCU
IAZ=14;NZ=14;IBZ=NZ;MZ=1;ICZ=NZ;IFAIL=0
CALL F04AAF(ZA,IAZ,ZB,IBZ,NZ,MZ,ZC,ICZ,WKSPCE,IFAIL)
DO 240 JUY=1,14;X(JUY)=ZC(JUY,1)
CONTINUE
TYPE*,(X(KI),KI=1,14)
G(15)=EXP(-X(1)*(E21*X(2)+E31*X(3)+E41*X(4)+E51*X(5)+E61*X(6)+
1E71*X(7))-(EA11*X(1)**2+EA22*X(2)**2+EA33*X(3)**2+EA44*X(4)**2+
1EA55*X(5)**2+EA66*X(6)**2+EA77*X(7)**2)/2.0)
G(16)=EXP(-X(8)*(E21*X(9)+E31*X(10)+E41*X(11)+E51*X(12)+E61
1*X(13)+E71*X(14))-(EF11*X(8)**2+EF22*X(9)**2+EF33*X(10)**2
1+EF44*X(11)**2+EF55*X(12)**2+EF66*X(13)**2+EF77*X(14)**2)/
12.0)
G(1)=EXP(EA11*X(1)+E21*X(2)+E31*X(3)+E51*X(5)+E61*X(6)+E71*X(7))
G(2)=EXP(E21*X(1)+EA22*X(2))
G(3)=EXP(E31*X(1)+EA33*X(3))
G(4)=EXP(E41*X(1)+EA44*X(4))
G(5)=EXP(E51*X(1)+EA55*X(5))
G(6)=EXP(E61*X(1)+EA66*X(6))
G(7)=EXP(E71*X(1)+EA77*X(7))
G(8)=EXP(EF11*X(8)+E21*X(9)+E31*X(10)+E41*X(11)+E51*X(12)+E61*
1X(13)+E71*X(14))
G(9)=EXP(E21*X(8)+EF22*X(2))
G(10)=EXP(E31*X(8)+EF33*X(10))
G(11)=EXP(E41*X(8)+EF44*X(11))
G(12)=EXP(E51*X(8)+EF55*X(12))
G(13)=EXP(E61*X(8)+EF66*X(13))
G(14)=EXP(E71*X(8)+EF77*X(14))
X(15)=(XC-X(1))/(X(8)-X(1))
XNEW=X(I)
IF(ABS(XOLD-XNEW)<=0.000001) GO TO 135
GO TO 129
CONTINUE

*****************************************************************

    * COMPOSITION CALCULATION IN LOCAL EQUILIBRIUM CONDITION *

*****************************************************************

XO(1)=XC*EXP(DOGC/(1.987*T))
```

```
      XL(2)=XMN*EXP(-DOGMN/(1.987*T))
      XL(3)=XSI*EXP(-DOGSI/(1.987*T))
      XL(4)=XNI*EXP(-DOGNI/(1.987*T))
      XL(5)=XCR*EXP(-DOGCR/(1.987*T))
      XL(6)=XMO*EXP(-DOGMO/(1.987*T))
      XL(7)=XCU*EXP(-DOGCU/(1.987*T))
      XL(8)=X(8)
      XL(9)=XMN
      XL(10)=XSI
      XL(11)=XNI
      XL(12)=XCR
      XL(13)=XMO
      XL(14)=XCU
      XFE=(1-XC-XMN-XSI-XNI-XCR-XMO-XCU)
      DO 192 I=1,14
193   XLOLD=XL(I)
      FL0=-DOGFE/(1.987*T)
     1-XL(1)*(E21*XL(2)+E31*XL(3)+E41*XL(4)+E51*XL(5)+E61*XL(6)+
     1E71*XL(7))-(EF11*XL(8)**2+EF22*XL(9)**2+EF33*XL(10)**2+EF44*
     1XL(11)**2+EF55*XL(12)**2+EF66*XL(13)**2+EF77*XL(14)**2)/2.0
      FL1=DOGC/(1.987*T)+(EF11*XL(8)+E21*XL(9)+E31*XL(10)+E41*XL(11)+
     1E51*XL(12)+E61*XL(13)+E71*XL(14))
      FL2=-DOGMN/(1.987*T)-(E21*XL(8)+EF22*XL(9))
      FL3=-DOGSI/(1.987*T)-(E31*XL(8)+EF33*XL(10))
      FL4=-DOGNI/(1.987*T)-(E41*XL(8)+EF44*XL(11))
      FL5=-DOGCR/(1.987*T)-(E51*XL(8)+EF55*XL(12))
      FL6=-DOGMO/(1.987*T)-(E61*XL(8)+EF66*XL(13))
      FL7=-DOGCU/(1.987*T)-(E71*XL(8)+EF77*XL(14))
      XL(1)=(1-XL(2)-XL(3)-XL(4)-XL(5)-XL(6)-XL(7))-(1-XL(8)-XL(9)-
     1XL(10)-XL(11)-XL(12)-XL(13)-XL(14))*EXP(FL0+XL(1)*(E21*XL(2)+
     1E31*XL(3)+E41*XL(4)+E51*XL(5)+E61*XL(6)+E71*XL(7))+(EA11*XL(1)
     1**2+EA22*XL(2)**2+EA33*XL(3)**2+EA44*XL(4)**2+EA55*XL(5)**2+
     1EF66*XL(6)**2+EF77*XL(7)**2)/2.0)
      XL(2)=XL(9)*EXP(FL2+EA22*XL(2)+E21*XL(1))
      XL(31)=XL(10)*EXP(FL3+EA33*XL(3)+E31*XL(1))
      XL(32)=XL(10)*EXP(FL3+EA33*XL(31)+E31*XL(1))
      XL(33)=XL(10)*EXP(FL3+EA33*XL(32)+E31*XL(1))
      IF(ABS(XL(33)-2.0*XL(32)+XL(31)).LT.0.000001) GO TO 197
      B=(XL(33)-XL(32))/(XL(33)-2.0*XL(32)+XL(31))
      XL(3)=B*XL(32)+(1.0-B)*XL(33)
      GO TO 198
197   XL(3)=XL(33)
198   XL(4)=XL(11)*EXP(FL4+EA44*XL(4)+E41*XL(1))
      XL(5)=XL(12)*EXP(FL5+EA55*XL(5)+E51*XL(1))
      XL(6)=XL(13)*EXP(FL6+EA66*XL(6)+E61*XL(1))
      XL(7)=XL(14)*EXP(FL7+EA77*XL(7)+E71*XL(1))
      XL(8)=XL(1)*EXP(FL1-(EF11*XL(8)+E21*XL(9)+E31*XL(10)+E41*XL(11)+
     1E51*XL(12)+E61*XL(13)+E71*XL(14)))
      XL(9)=XMN*(1-XL(8)-XL(10)-XL(11)-XL(12)-XL(13)-XL(14))/(XFE+XMN)
      XL(10)=XSI*(1-XL(8)-XL(9)-XL(11)-XL(12)-XL(13)-XL(14))/(XFE+XSI)
      XL(11)=XNI*(1-XL(8)-XL(9)-XL(10)-XL(12)-XL(13)-XL(14))/(XFE+XNI)
      XL(12)=XCR*(1-XL(8)-XL(9)-XL(10)-XL(11)-XL(13)-XL(14))/(XFE+XCR)
      XL(13)=XMO*(1-XL(8)-XL(9)-XL(10)-XL(11)-XL(12)-XL(14))/(XFE+XMO)
      XL(14)=XCU*(1-XL(8)-XL(9)-XL(10)-XL(11)-XL(12)-XL(13))/(XFE+XCU)
      XLNEW=XL(1)
      IF(ABS(XLOLD-XLNEW).LT.0.000001) GO TO 196
      GO TO 193
192   CONTINUE
196   AC=XL(1)*EXP(EA11*XL(1)+E21*XL(2)+E31*XL(3)+E41*XL(4)+E51*XL(5)
     1+E61*XL(6)+E71*XL(7))
      XN(1)=XL(1)
      XN(2)=XL(9)
      XN(3)=XL(10)
      XN(4)=XL(11)
      XN(5)=XL(12)
      XN(6)=XL(13)
      XN(7)=XL(14)
      DO 169 I=1,7
170   XOLD1=XN(1)
      XN(1)=AC*EXP(-(EA11*XN(1)+E21*XN(2)+E31*XN(3)+E41*XN(4)+E51
     1*XN(5)+E61*XN(6)+E71*XN(7)))
      XN(2)=X(9)*(1-XN(1)-XN(3)-XN(4)-XN(5)-XN(6)-XN(7))/(1-X(8)-X(10)
     1-X(11)-X(12)-X(13)-X(14))
      XN(3)=X(10)*(1-XN(1)-XN(2)-XN(4)-XN(5)-XN(6)-XN(7))/(1-X(8)-X(9)
     1-X(11)-X(12)-X(13)-X(14))
```

```
XN(4)=X(11)*(1-XN(1)-XN(2)-XN(3)-XN(5)-XN(6)-XN(7))/(1-X(8)-X(9)
1-X(10)-X(12)-X(13)-X(14))
XN(5)=X(12)*(1-XN(1)-XN(2)-XN(3)-XN(4)-XN(6)-XN(7))/(1-X(8)-X(9)
1-X(10)-X(11)-X(13)-X(14))
XN(6)=X(13)*(1-XN(1)-XN(2)-XN(3)-XN(4)-XN(5)-XN(7))/(1-X(8)-X(9)
1-X(10)-X(11)-X(12)-X(14))
XN(7)=X(14)*(1-XN(1)-XN(2)-XN(3)-XN(4)-XN(5)-XN(6))/(1-X(8)-X(9)
1-X(10)-X(11)-X(12)-X(13))
XNEW1=XN(1)
IF(ABS(XOLD1-XNEW1).LE.0.000001) GO TO 171
GO TO 170
CONTINUE
WRITE(22,144)
FORMAT(16X,1HO,3X,'EA11',5X,'EA22',5X,'EA33',5X,'EA44',5X,'EA55'
1,5X,'EA66',5X,'EA77')
WRITE(22,145),EA11,EA22,EA33,EA44,EA55,EA66,EA77
FORMAT(16X,1HO,7(F8.4,1X)/)
WRITE(22,150)
FORMAT(16X,1HO,3X,'EF11',5X,'EF22',5X,'EF33',5X,'EF44',5X,'EF55'
1,5X,'EF66',5X'EF77')
WRITE(22,151)EF11,EF22,EF33,EF44,EF55,EF66,EF77
FORMAT(16X,1HO,7(F8.4,1X)/)
WRITE(22,152)
FORMAT(16X,1HO,3X,'E21',6X,'E31',6X,'E41',6X,'E51',6X,'E61',6X,
1'E71')
WRITE(22,153)E21,E31,E41,E51,E61,E71
FORMAT(16X,1HO,6(F8.4,1X)/)
WRITE(22,138)
FORMAT(16X,1HO,4X,'DOGFe',8X,'DOGC',8X,'DOGMn',8X,'DOGSi',8X,
1'DOGNi')
WRITE(22,139),DOGFE,DOGC,DOGMN,DOGSI,DOGNI
FORMAT(16X,1HO,4(F11.5,2X),F10.4/)
WRITE(22,154)
FORMAT(16X,1HO,4X,'DOGCr',8X,'DOGMo',7X,'DOGCu')
WRITE(22,155)DOGCR,DOGMO,DOGCU
FORMAT(16X,1HO,3(F11.5,2X)/)
WRITE(22,142)
FORMAT(16X,1HO,3X,'XAC',6X,'XAMn',5X,'XASi',5X,'XANi',5X,'XACr'
1,5X,'XAMo',5X,'XACu')
WRITE(22,131)(X(I),I=1,7)
FORMAT(16X,1HO,7(F8.6,1X)/)
WRITE(22,158)
FORMAT(16X,1HO,3X,'XFC',6X,'XFMn',5X,'XFSi',5X,'XFNi',5X,'XFCr'
1,5X,'XFMo',5X,'XFCu')
WRITE(22,159)(X(I),I=8,14)
FORMAT(16X,1HO,7(F8.6,1X)/)
WRITE(22,204)
FORMAT(16X,1HO,3X,'XLC',6X,'XLMn',5X,'XLSi',5X,'XLNi',5X,'XLCr'
1,5X,'XLMo',5X,'XLCu')
WRITE(22,205)(XL(I),I=1,7)
FORMAT(16X,1HO,7(F8.6,1X)/)
WRITE(22,206)
FORMAT(16X,1HO,3X,'X1C',6X,'X1Mn',5X,'X1Si',5X,'X1Ni',5X,'X1Cr'
1,5X,'X1Mo',5X,'X1Cu')
WRITE(22,207)(XL(I),I=8,14)
FORMAT(16X,1HO,7(F8.6,1X)/)
WRITE(22,172)
FORMAT(16X,1HO,3X,'XNC',6X,'XNMn',5X,'XNSi',5X,'XNNi',5X,'XNCr'
1,5X,'XNMo',5X,'XNCu')
WRITE(22,173)(XN(I),I=1,7)
FORMAT(16X,1HO,7(F8.6,1X)/)
VLALPH=(XC-XN(1))/(XL(8)-XN(1))
VMTNSI=1.-X(15)
VLMNSI=1.-VLALPH
TYPE*,VMTNST,VLMNST
WRITE(22,190)
FORMAT(16X,1HO,2X,'Valpha',5X,'VLalpha',6X,'VMTNSI',6X,'VLMNST',
16X,'AC')
WRITE(22,191)X(15),VLALPH,VMTNSI,VLMNST,AC
FORMAT(16X,1HO,5(F8.6,4X)/)
V2=(XMN-XN(2))/(XL(9)-XN(2))
V3=(XST-XN(3))/(XL(10)-XN(3))
V4=(XNI-XN(4))/(XL(11)-XN(4))
V5=(XCR-XN(5))/(XL(12)-XN(5))
V6=(XMO-XN(6))/(XL(13)-XN(6))
V7=(XCU-XN(7))/(XL(14)-XN(7))
```

```
      WRITE(22,208)
208   FORMAT(16X,1HO,'VLalpha1',1X,'VLalpha2',1X,'VLalpha3',1X,
     1'VLalpha4',1X,'VLalpha5',1X,'VLalpha6',1X,'VLalpha7')
      WRITE(22,209)VLALPH,V2,V3,V4,V5,V6,V7
209   FORMAT(16X,1HO,7(F8.5,1X)/)
C     ****************************************************************
C      CALCULATIONS OF PERCENTAGES OF VARIOUS ELEMENTS IN FERRITE AND
C                AUSTENITE IN COMPLETE EQUILIBRIUM CONDITION
C     ****************************************************************
      DX1=X(1)*12.011+X(2)*54.938+X(3)*28.086+X(4)*58.71+X(5)*51.996
     1+X(6)*95.94+X(7)*63.64+(1-X(1)-X(2)-X(3)-X(4)-X(5)-X(6)-X(7))
     1*55.847
      DX2=X(8)*12.011+X(9)*54.938+X(10)*28.086+X(11)*58.71+X(12)*
     151.996+X(13)*95.94+X(14)*63.54+(1-X(8)-X(9)-X(10)-X(11)-X(12)
     1-X(13)-X(14))*55.847
      PAC=100.0*(X(1)*12.011)/DX1
      PAMN=100.0*(X(2)*54.938)/DX1
      PASI=100.0*(X(3)*28.086)/DX1
      PANI=100.0*(X(4)*58.71)/DX1
      PACR=100.0*(X(5)*51.996)/DX1
      PAMO=100.0*(X(6)*95.94)/DX1
      PACU=100.0*(X(7)*63.54)/DX1
      PFC=100.0*(X(8)*12.011)/DX2
      PFMN=100.0*(X(9)*54.938)/DX2
      PFSI=100.0*(X(10)*28.086)/DX2
      PFNI=100.0*(X(11)*58.71)/DX2
      PFCR=100.0*(X(12)*51.996)/DX2
      PFMO=100.0*(X(13)*95.94)/DX2
      PFCU=100.0*(X(14)*63.54)/DX2
      DXL1=XL(1)*12.011+XL(2)*54.938+XL(3)*28.086+XL(4)*58.71+XL(5)*
     151.996+XL(6)*95.94+XL(7)*63.64+(1-XL(1)-XL(2)-XL(3)-XL(4)-XL(5)
     1-XL(6)-XL(7))*55.847
      DXL2=XL(8)*12.011+XL(9)*54.938+XL(10)*28.086+XL(11)*58.71+XL(12)
     1*51.996+XL(13)*95.94+XL(14)*63.54+(1-XL(8)-XL(9)-XL(10)-XL(11)-
     1XL(12)-XL(13)-XL(14))*55.847
      PLC=100.0*(XL(1)*12.011)/DXL1
      PLMN=100.0*(XL(2)*54.938)/DXL1
      PLSI=100.0*(XL(3)*28.086)/DXL1
      PLNI=100.0*(XL(4)*58.71)/DXL1
      PLCR=100.0*(XL(5)*51.996)/DXL1
      PLMO=100.0*(XL(6)*95.94)/DXL1
      PLCU=100.0*(XL(7)*63.54)/DXL1
      PL1C=100.0*(XL(8)*12.011)/DXL2
      PL1MN=100.0*(XL(9)*54.938)/DXL2
      PL1SI=100.0*(XL(10)*28.086)/DXL2
      PL1NI=100.0*(XL(11)*58.71)/DXL2
      PL1CR=100.0*(XL(12)*51.996)/DXL2
      PL1MO=100.0*(XL(13)*95.94)/DXL2
      PL1CU=100.0*(XL(14)*63.54)/DXL2
      DXN1=XN(1)*12.011+XN(2)*54.938+XN(3)*28.086+XN(4)*58.71+XN(5)*
     151.996+XN(6)*95.94+XN(7)*63.64+(1-XN(1)-XN(2)-XN(3)-XN(4)-XN(5)
     1-XN(6)-XN(7))*55.847
      PNC=100.0*(XN(1)*12.011)/DXN1
      PNMN=100.0*(XN(2)*54.938)/DXN1
      PNSI=100.0*(XN(3)*28.086)/DXN1
      PNNI=100.0*(XN(4)*58.71)/DXN1
      PNCR=100.0*(XN(5)*51.996)/DXN1
      PNMO=100.0*(XN(6)*95.94)/DXN1
      PNCU=100.0*(XN(7)*63.54)/DXN1
      WRITE(22,143)
143   FORMAT(16X,1HO,3X,'PAC',5X,'PAMn',6X,'PASi',5X,'PANi',5X,'PACr'
     1,5X,'PAMo',5X,'PACu')
      WRITE(22,132)PAC,PAMN,PASI,PANI,PACR,PAMO,PACU
132   FORMAT(16X,1HO,7(F8.6,1X)/)
      WRITE(22,160)
160   FORMAT(16X,1HO,3X,'PFC',6X,'PFMn',5X,'PFSi',5X,'PFNi',5X,'PFCr'
     1,5X,'PFMo',5X,'PFCu')
      WRITE(22,161)PFC,PFMN,PFSI,PFNI,PFCR,PFMO,PFCU
161   FORMAT(16X,1HO,7(F8.6,1X)/)
```

```
WRITE(22,162)
FORMAT(16X,1HO,3X,'PLC',6X,'PLMn',5X,'PLSi',5X,'PLNi',5X,'PLCr'
1,5X,'PLMo',5X,'PLCu')
WRITE(22,163)PLC,PLMN,PLSI,PLNI,PLCR,PLMO,PLCU
FORMAT(16X,1HO,7(F8.6,1X)/)
WRITE(22,133)
FORMAT(16X,1HO,3X,'P1C',5X,'P1Mn',6X,'P1Si',5X,'P1Ni',5X,'P1Cr'
1,5X,'P1Mo',5X,'P1Cu')
WRITE(22,134)PL1C,PL1MN,PL1SI,PL1NI,PL1CR,PL1MO,PL1CU
FORMAT(16X,1HO,7(F8.6,1X)/)
WRITE(22,136)
FORMAT(16X,1HO,3X,'PNC',6X,'PNMn',5X,'PNSi',5X,'PNNi',5X,'PNCr'
1,5X,'PNMO',5X,'PNCU')
WRITE(22,137)PNC,PNMN,PNSI,PNNI,PNCR,PNMO,PNCU
FORMAT(16X,1HO,7(F8.6,1X)/)
CLOSE(UNIT=22,FILE='COM.DAT')
CONTINUE
STOP
END
```

APPENDIX III

```
C     ****************************************************************
C     *  PROGRAM FOR COMPUTATION OF AE3 TEMPERATURE IN               *
C     *                COMPLETE EQUILIBRIUM CONDITION *              *
C     ****************************************************************
      DIMENSION TEMP(57),DSGFE(57),X(15),XN(7),XL(14),G(16)
      DIMENSION ZA(14,14),ZB(14,1),ZC(14,1),WKSPCE(200)
      OPEN(UNIT=22,FILE='COM.DAT')
      DO 100 K=1,57
100   READ(*,*)TEMP(K),DSGFE(K)
      CONTINUE
      NS=1
      DO 101 L=1,NS
      READ(*,*)PC,PMN,PSI,PNI,PCR,PMO,PCU
      T=0.0001
C     ****************************************************************
C     *                  * MOLE FRACTION CALCULATIONS *              *
C     ****************************************************************
      WRITE(22,103)
103   FORMAT('////16X,'COMPUTATION OF MOLE FRACTIONS OF STEEL IN FERRIT
     1E AND AUSTENITE'/ )
      WRITE(22,104)
104   FORMAT(16X,1HO,8X,'* COMPOSITION OF STEEL IN WEIGHT PERCENTAGE *
     1'/)
      WRITE(22,108)
108   FORMAT(16X,1HO,3X,'C',6X,'Mn',7X,'Si',6X,'Ni',6X,'Cr',6X,'Mo',6X
     1,'Cu',4X,'Temp')
      WRITE(22,105)PC,PMN,PSI,PNI,PCR,PMO,PCU,T
105   FORMAT(16X,1HO,7(F6.4,2X),F6.1/)
      WRITE(22,107)
107   FORMAT(16X,1HO,4X,'XC',6X,'XMn',6X,'XSi',6X,'XNi',6X,'XCr',6X,
     1'XMo',6X,'XCu')
      DENMX=(100.0-PC-PMN-PSI-PNI-PCR-PMO-PCU)/55.847+PC/12.011
     1+PMN/54.938+PSI/28.086+PNI/58.71+PCR/51.996+PMO/95.94+PCU/63.54
109   IF(PC.EQ.0.0) GO TO 110
      XC=(PC/12.011)/DENMX
      GO TO 111
110   XC=10.0E-9
111   IF(PMN.EQ.0.0) GO TO 112
      XMN=(PMN/54.938)/DENMX
      GO TO 113
112   XMN=10.0E-9
113   IF(PSI.EQ.0.0) GO TO 114
      XSI=(PSI/28.086)/DENMX
      GO TO 115
114   XSI=10.0E-9
115   IF(PNI.EQ.0.0) GO TO 116
      XNI=(PNI/58.71)/DENMX
      GO TO 117
116   XNI=10.0E-9
117   IF(PCR.EQ.0.0) GO TO 118
      XCR=(PCR/51.996)/DENMX
      GO TO 119
118   XCR=10.0E-9
119   IF(PMO.EQ.0.0) GO TO 120
      XMO=(PMO/95.94)/DENMX
      GO TO 121
120   XMO=10.0E-9
121   IF(PCU.EQ.0.0) GO TO 122
      XCU=(PCU/63.54)/DENMX
      GO TO 123
122   XCU=10.0E-9
123   WRITE(22,124)XC,XMN,XSI,XNI,XCR,XMO,XCU
124   FORMAT(16X,1HO,7(F8.5,1X)/)
```

```
************************************************************************
      CALCULATION OF AE3 TEMPERATURE IN COMPLETE EQUILIBRIUM
************************************************************************

TEMP=1000.0
N=1
INDER=1
GO TO 175
INDER=2
T=TEMP+FLOAT(INDER)*H
I=K
I=1
I=I+1
IF(T-TEMP(I)) 126,126,125
DSGFE=DSGFE(I-1)+(DSGFE(I)-DSGFE(I-1))*(T-TEMP(I-1))/(TEMP(I)
1-TEMP(I-1))

************************************************************************
              * INTERACTION PARAMETER CALCULATIONS *
************************************************************************

EA11=8910.0/T
EA21=-4050.0/T
EA22=220.0/T
EA31=12650.0/T
EA33=(-3059.0/T)-41.0377+9.9873*ALOG(T)
EA41=5170.0/T
EA44=-1870.0/T
EA51=-14080.0/T
EA55=330.0/T
EA61=-10670.0/T
EA66=-2310.0/T
EA71=4180.0/T
EA77=-7260.0/T
EE11=0.0
EE22=-990.0/T
EE33=(-21787.0/T)+6.4544+5.2320*ALOG(T)
EE44=-1870.0/T
EE55=-2970.0/T
EE66=-4290.0/T
EE77=-8910.0/T

************************************************************************
              * CALCULATION OF CHANGE IN FREE ENERGY *
************************************************************************

DGGC=7.6866*T-15323.0
DGGMN=-38795.0+62.137*T-0.0255*((T)**2)
DGGSI=-5964.0+38.7996*T-4.7244*T*ALOG(T)
DGGNI=3.233*T-4545.0
DGGCR=-367.0-4.656*T+0.6568*T*ALOG(T)
DGGMO=565.0+0.15*T
DGGCU=-0.017*((T)**2)+41.183*T-25500.0

************************************************************************
  * COMPOSITION CALCULATIONS IN COMPLETE EQUILIBRIUM CONDITION *
************************************************************************

X(1)=XC
X(2)=XMN
X(3)=XSI
X(4)=XNI
X(5)=XCR
```

```
Y(6)=XMN
Y(7)=XSI
Y(8)=XNI*EXP(DJGSI/(1.987*T))
Y(9)=XMN*EXP(DJGMN/(1.987*T))
Y(10)=XSI*EXP(DJGSI/(1.987*T))
Y(11)=XNI*EXP(DJGNI/(1.987*T))
Y(12)=XCR*EXP(DJGCR/(1.987*T))
Y(13)=XMO*EXP(DJGMO/(1.987*T))
Y(14)=XCU*EXP(DJGCU/(1.987*T))
DO 130 I=8,15
X(I)=Y(I)
FO=-DJGFE/(1.987*T)
1-X(8)*(EF21*X(9)+EF31*X(10)+EF41*X(11)+EF51*X(12)+EF61*X(13)+EF71*
1X(14))-(EF11*X(8)**2+EF22*X(9)**2+EF33*X(10)**2+EF44*X(11)**2+
1EF55*X(12)**2+EF66*X(13)**2+EF77*X(14)**2)/2.0
F1=DJGFE/(1.987*T)+EA11*X(1)+EF21*X(2)+EF31*X(3)+EF41*X(4)+EF51*X(5)
1+EF61*X(6)+EF71*X(7)
F2=DJGMN/(1.987*T)+EF21*X(1)+EA22*X(2)
F3=DJGSI/(1.987*T)+EF31*X(1)+EA33*X(3)
F4=DJGNI/(1.987*T)+EF41*X(1)+EA44*X(4)
F5=DJGCR/(1.987*T)+EF51*X(1)+EA55*X(5)
F6=DJGMO/(1.987*T)+EF61*X(1)+EA66*X(6)
F7=DJGCU/(1.987*T)+EF71*X(1)+EA77*X(7)
X(1)=(1-X(1)-X(2)-X(3)-X(4)-X(5)-X(6)-X(7))-(1-X(8)-X(9)-X(10)
1-X(11)-X(12)-X(13)-X(14))*EXP(F0+X1*(EF21*X(2)+EF31*X(3)+EF41*X(4)
1+EF51*X(5)+EF61*X(6)+EF71*X(7))+(EA11*X(1)**2+EA22*X(2)**2+EA33*
1X(3)**2+EA44*X(4)**2+EA55*X(5)**2+EA66*X(6)**2+EA77*X(7)**2)/2)
X(8)=X(1)*EXP(F1-EF11*X(8)-EF21*X(9)-EF31*X(10)-EF41*X(11)-EF51*
1X(12)+EF61*X(13)+EF71*X(14))
X(9)=X(2)*EXP(F2-EF22*X(9)-EF21*X(8))
X(101)=X(3)*EXP(F3-EF33*X(10)-EF31*X(8))
X(102)=X(3)*EXP(F3-EF33*X(101)-EF31*X(8))
X(103)=X(3)*EXP(F3-EF33*X(102)-EF31*X(8))
IF(ABS(X(103)-2.0*X(102)+X(101)).LT.0.000001) GO TO 148
A=(X(103)-X(102))/(X(103)-2.0*X(102)+X(101))
X(10)=A*X(102)+(1.0-A)*X(103)
GO TO 149
X(10)=X(103)
X(11)=X(4)*EXP(F4-EF44*X(11)-EF41*X(8))
X(12)=X(5)*EXP(F5-EF55*X(12)-EF51*X(8))
X(13)=X(6)*EXP(F6-EF66*X(13)-EF61*X(8))
X(14)=X(7)*EXP(F7-EF77*X(14)-EF71*X(8))
XNEW=X(1)
IF(ABS(XOLD-XNEW)<=0.000001) GO TO 135
GO TO 129
CONTINUE
FT=DJGFE/(1.987*T)+ALOG(1-XC-XMN-XSI-XNI-XCR-XMO-XCU)-XC*(EF21*
1XMN+EF31*XSI+EF41*XNI+EF51*XCR+EF61*XMO+EF71*XCU)+(EF22*XMN**2+EF33*
1XSI**2+EF44*XNI**2+EF55*XCR**2+EF66*XMO**2+EF77*XCU**2)/2.0
FUNN=FT-ALOG(1-X(1)-X(2)-X(3)-X(4)-X(5)-X(6)-X(7))+X(1)*
1(EF21*X(2)+EF31*X(3)+EF41*X(4)+EF51*X(5)+EF61*X(6)+EF71*X(7))
1-(EA11*X(1)**2+EA22*X(2)**2+EA33*X(3)**2+EA44*X(4)**2+EA55
1*X(5)**2+EA66*X(6)**2+EA77*X(7)**2)/2.0
IF (INDER.EQ.2) GO TO 177
FUNA=FUNN
GO TO 176
FUNB=FUNN
FUNI=(FUNA+FUNB)/2.0
DFUNT=(FUNB-FUNA)/H
TNEW=T-(FUNI/DFUNT)
IF (ABS(T-TNEW).LT.1) GO TO 178
GO TO 179
CONTINUE
AUSIC=TNEW-273.
WRITE(22,195)
FORMAT(16X,1HO,2X,'PARTITIONING TEMPERATURE IN COMPLETE
1EQUILIBRIUM CONDITION')
WRITE(22,180)TNEW,AUSIC
FORMAT(16X,1HO,' THE PARTITTIONING AE3 TEMPERATURE IS = ',
1F6.1,' DEGREES KELVIN'//16X,1HO,38X,'= ',F6.1,' DEGS
1CENTIGRADE')
```

```
      GO TO 181
179   IF (N.GT.10) GO TO 182
      N=N+1
      T=TNEW
      GO TO 174
182   WRITE(22,183)
183   FORMAT(15X,'THE PROGRAM FAILS TO CONVERGE ')
      GO TO 101
181   CONTINUE
      TYPE*,EF,FUAN,FUNA,FUNB,FUNT,DFUNT
      TYPE*,TNEW,AUSTC,I,N
      CLOSE(UNIT=22,FILE='COM.DAT')
101   CONTINUE
      STOP
      END
```

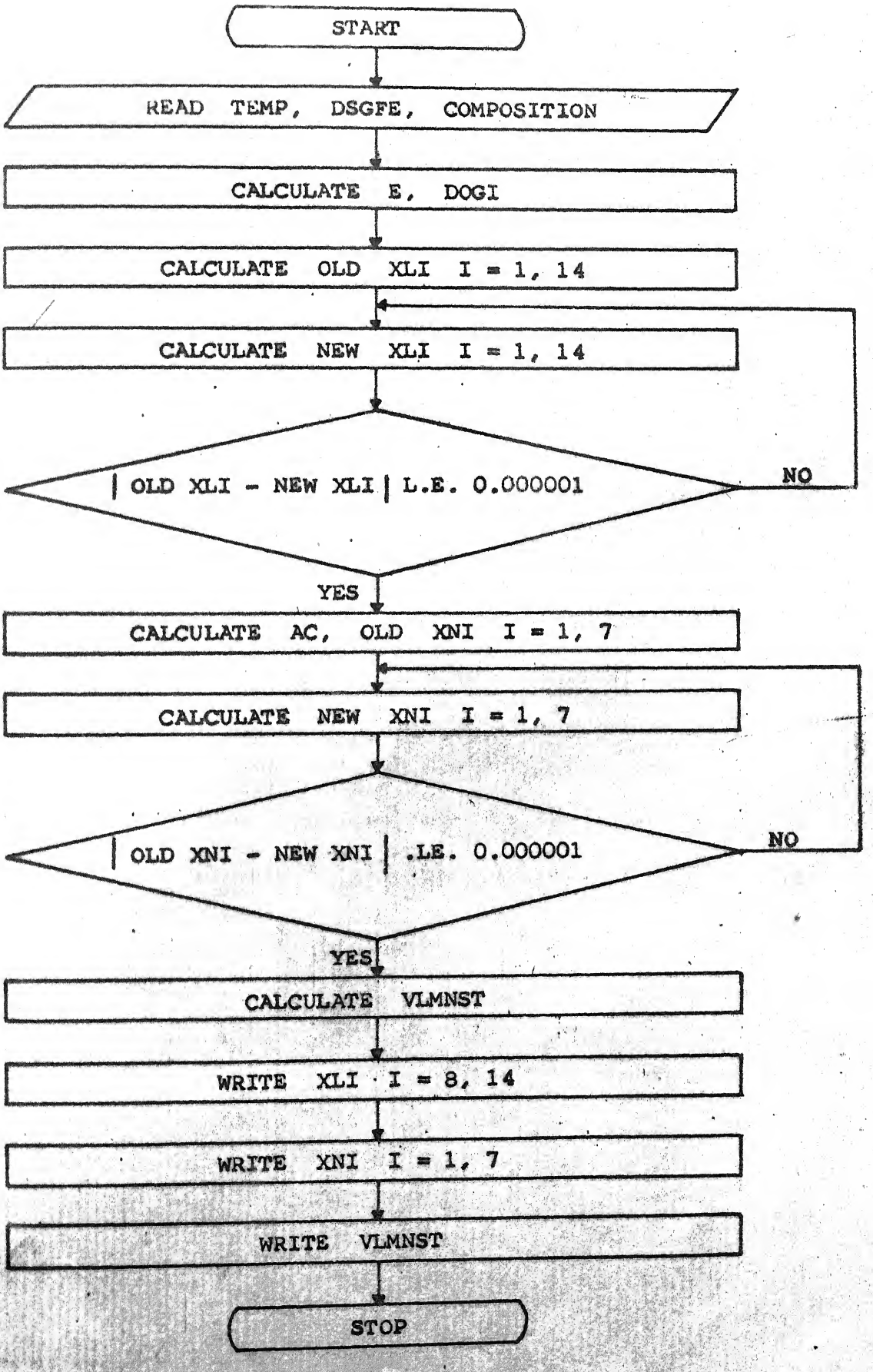

The flow chart for the calculation of martensite volume fraction in local equilibrium no-partition condition.

APPENDIX IV

```
C*****************************************************************
C     * PROGRAM FOR COMPUTATION OF ELEMENTAL COMPOSITION OF DUAL
C       PHASE STEELS IN FERRITE AND AUSTENITE SEPERATELY *
C*****************************************************************
      DIMENSION TEMP(57),DSGFE(57),X(15),XN(7),XL(14),XB(14),G(16)
      DIMENSION ZA(14,14),ZB(14,1),ZC(14,1),WKSPCE(200)
      OPEN(UNIT=22,FILE='COM.DAT')
      DO 100 K=1,57
      READ*,TEMP(K),DSGFE(K)
  100 CONTINUE
      NS=1
      DO 101 L=1,NS
      READ*,PC,PMN,PSI,PNI,PCR,PMO,PCU,T
C*****************************************************************
C                  * MOLE FRACTION CALCULATIONS *
C*****************************************************************
      WRITE(22,103)
  103 FORMAT(////16X,'COMPUTATION OF MOLE FRACTIONS OF STEEL IN FERRIT
     1E AND A'STENITE'/ )
      WRITE(22,104)
  104 FORMAT(15X,1H0,8X,'* COMPOSITION OF STEEL IN WEIGHT PERCENTAGE *
     1'/)
      WRITE(22,108)
  108 FORMAT(15X,1H0,3X,'C',6X,'Mn',7X,'Si',6X,'Ni',6X,'Cr',6X,'Mo',6X
     1,'Cu',4X,'Temp')
      WRITE(22,105)PC,PMN,PSI,PNI,PCR,PMO,PCU,T
  105 FORMAT(15X,1H0,7(F6.4,2X),F6.1/)
      WRITE(22,107)
  107 FORMAT(16X,1H0,4X,'XC',6X,'XMN',6X,'XSI',6X,'XNI',6X,'XCr',6X,
     1'XMO',6X,'XCu')
      DENMX=(100.0-PC-PMN-PSI-PNI-PCR-PMO-PCU)/55.847+PC/12.011
     1+PMN/54.938+PSI/28.086+PNI/58.71+PCR/51.996+PMO/95.94+PCU/63.54
      IF(PC.EQ.0.0) GO TO 110
      XC=(PC/12.011)/DENMX
      GO TO 111
  110 XC=10.0E-9
  111 IF(PMN.EQ.0.0) GO TO 112
      XMN=(PMN/54.938)/DENMX
      GO TO 113
  112 XMN=10.0E-9
  113 IF(PSI.EQ.0.0) GO TO 114
      XSI=(PSI/28.086)/DENMX
      GO TO 115
  114 XSI=10.0E-9
  115 IF(PNI.EQ.0.0) GO TO 116
      XNI=(PNI/58.71)/DENMX
      GO TO 117
  116 XNI=10.0E-9
  117 IF(PCR.EQ.0.0) GO TO 118
      XCR=(PCR/51.996)/DENMX
      GO TO 119
  118 XCR=10.0E-9
  119 IF(PMO.EQ.0.0) GO TO 120
      XMO=(PMO/95.94)/DENMX
      GO TO 121
  120 XMO=10.0E-9
  121 IF(PCU.EQ.0.0) GO TO 122
      XCU=(PCU/63.54)/DENMX
      GO TO 123
  122 XCU=10.0E-9
  123 WRITE(22,124)XC,XMN,XSI,XNI,XCR,XMO,XCU
  124 FORMAT(16X,1H0,7(F8.6,1X)/)
      I=K
      I=1
      I=I+1
      IF(I-TEMP(I)) 126,126,125
```

```
DDGFE=DSGFE(I-1)+(DSGFE(J)-DSGFE(J-1))*(T-TEMP(J-1))/(TEMP(J)
1-TEMP(J-1))

*****************************************************************

            * INTERACTION PARAMETER CALCULATIONS *

*****************************************************************

EA11=8910.0/T
E21=-4950.0/T
EA22=220.0/T
E31=12650.0/T
EA33=(-30690.0/T)-41.0377+9.9873*ALOG(T)
E41=5170.0/T
EA44=-1870.0/T
E51=-11080.0/T
EA55=330.0/T
E61=-10670.0/T
EA66=-2310.0/T
E71=4180.0/T
EA77=-7260.0/T
EF11=0.0
EF22=-990.0/T
EF33=(-21787.0/T)+6.4544+5.2320*ALOG(T)
EF44=-1870.0/T
EF55=-2970.0/T
EF66=-4290.0/T
EF77=-8910.0/T

*****************************************************************

            * CALCULATION OF CHANGE IN FREE ENERGY *

*****************************************************************

DDGC=7.6866*T-15323.0
DDGMN=-38795.0+62.137*T-0.0255*((T)**2)
DDGSI=-5964.0+38.7996*T-4.7244*T*ALOG(T)
DDGNI=3.233*T-4545.0
DDGCR=-367.0-4.656*T+0.6568*T*ALOG(T)
DDGMO=565.0+0.15*T
DDGCU=-0.017*((T)**2)+41.183*T-25500.0

*****************************************************************

   * COMPOSITION CALCULATION IN LOCAL EQUILIBRIUM CONDITION *

*****************************************************************

XL(1)=XC*EXP(DDGC/(1.987*T))
XL(2)=XMN*EXP(-DDGMN/(1.987*T))
XL(3)=XSI*EXP(-DDGSI/(1.987*T))
XL(4)=XNI*EXP(-DDGNI/(1.987*T))
XL(5)=XCR*EXP(-DDGCR/(1.987*T))
XL(6)=XMO*EXP(-DDGMO/(1.987*T))
XL(7)=XCU*EXP(-DDGCU/(1.987*T))
XL(8)=XC*EXP(DDGC/(1.987*T))
XL(9)=XMN
XL(10)=XSI
XL(11)=XNI
XL(12)=XCR
XL(13)=XMO
XL(14)=XCU
XFE=(1-XC-XMN-XSI-XNI-XCR-XMO-XCU)
DO 192 I=1,14
XLOLD=XL(I)
FLO=-DDGFE/(1.987*T)
1-XL(1)*(E21*XL(2)+E31*XL(3)+E41*XL(4)+E51*XL(5)+E61*XL(6)+
1E71*XL(7))-(EF11*XL(8)**2+EF22*XL(9)**2+EF33*XL(10)**2+EF44*
1F71*XL(7))-(EF11*XL(8)**2+EF22*XL(9)**2+EF33*XL(10)**2+EF44*
1XL(11)**2+EF55*XL(12)**2+EF66*XL(13)**2+EF77*XL(14)**2)/2.0
FL1=DDGFE/(1.987*T)+(EF11*XL(8)+E21*XL(9)+E31*XL(10)+E41*XL(11)+
1E51*XL(12)+E61*XL(13)+E71*XL(14))
```

```
FL2=-DG*XMN/(1.987*T)-(E21*XL(8)+EF22*XL(9))
FL3=-DG*XSI/(1.987*T)-(E31*XL(8)+EF33*XL(10))
FL4=-DG*XNI/(1.987*T)-(E41*XL(8)+EF44*XL(11))
FL5=-DG*XCR/(1.987*T)-(E51*XL(8)+EF55*XL(12))
FL6=-DG*XMO/(1.987*T)-(E61*XL(8)+EF66*XL(13))
FL7=-DG*XCU/(1.987*T)-(E71*XL(8)+EF77*XL(14))
XL(1)=(1-XL(2)-XL(3)-XL(4)-XL(5)-XL(6)-XL(7))-(1-XL(8)-XL(9)-
1XL(10)-XL(11)-XL(12)-XL(13)-XL(14))*EXP(FL0+XL(1)*(E21*XL(2)+
1E31*XL(3)+E41*XL(4)+E51*XL(5)+E61*XL(6)+E71*XL(7))+(EA11*XL(1)
1**2+EA22*XL(2)**2+EA33*XL(3)**2+EA44*XL(4)**2+EA55*XL(5)**2+
1EA66*XL(6)**2+EF77*XL(7)**2)/2.0)
XL(2)=XL(9)*EXP(FL2+EA22*XL(2)+E21*XL(1))
XL(31)=XL(10)*EXP(FL3+EA33*XL(3)+E31*XL(1))
XL(32)=XL(10)*EXP(FL3+EA33*XL(31)+E31*XL(1))
XL(33)=XL(10)*EXP(FL3+EA33*XL(32)+E31*XL(1))
IF(ABS(XL(33)-2.0*XL(32)+XL(31)).LT.0.000001) GO TO 197
R=(XL(33)-XL(32))/(XL(33)-2.0*XL(32)+XL(31))
XL(3)=R*XL(32)+(1.0-R)*XL(33)
GO TO 198
XL(3)=XL(33)
XL(4)=XL(11)*EXP(FL4+EA44*XL(4)+E41*XL(1))
XL(5)=XL(12)*EXP(FL5+EA55*XL(5)+E51*XL(1))
XL(6)=XL(13)*EXP(FL6+EA66*XL(6)+E61*XL(1))
XL(7)=XL(14)*EXP(FL7+EA77*XL(7)+E71*XL(1))
XL(8)=XL(1)*EXP(FL1-(EF11*XL(8)+E21*XL(9)+E31*XL(10)+E41*XL(11)+
1E51*XL(12)+E61*XL(13)+E71*XL(14)))
XL(9)=XMN*(1-XL(8)-XL(10)-XL(11)-XL(12)-XL(13)-XL(14))/(XFE+XMN)
XL(10)=XSI*(1-XL(8)-XL(9)-XL(11)-XL(12)-XL(13)-XL(14))/(XFE+XSI)
XL(11)=XNI*(1-XL(8)-XL(9)-XL(10)-XL(12)-XL(13)-XL(14))/(XFE+XNI)
XL(12)=XCR*(1-XL(8)-XL(9)-XL(10)-XL(11)-XL(13)-XL(14))/(XFE+XCR)
XL(13)=XMO*(1-XL(8)-XL(9)-XL(10)-XL(11)-XL(12)-XL(14))/(XFE+XMO)
XL(14)=XCU*(1-XL(8)-XL(9)-XL(10)-XL(11)-XL(12)-XL(13))/(XFE+XCU)
XLNEW=XL(1)
IF(ABS(XLOLD-XLNEW).LT.0.000001) GO TO 196
GO TO 193
CONTINUE
AC=XL(1)*EXP(EA11*XL(1)+E21*XL(2)+E31*XL(3)+E41*XL(4)+E51*XL(5)
1+E61*XL(6)+E71*XL(7))
XN(1)=XL(1)
XN(2)=XL(9)
XN(3)=XL(10)
XN(4)=XL(11)
XN(5)=XL(12)
XN(6)=XL(13)
XN(7)=XL(14)
DO 169 I=1,7
XOLD1=XN(I)
XN(1)=AC*EXP(-(EA11*XN(1)+E21*XN(2)+E31*XN(3)+E41*XN(4)+E51
1*XN(5)+E61*XN(6)+E71*XN(7)))
XN(2)=XL(9)*(1-XN(1)-XN(3)-XN(4)-XN(5)-XN(6)-XN(7))/(1-XL(8)-
1XL(10)-XL(11)-XL(12)-XL(13)-XL(14))
XN(3)=XL(10)*(1-XN(1)-XN(2)-XN(4)-XN(5)-XN(6)-XN(7))/(1-XL(8)-
1XL(9)-XL(11)-XL(12)-XL(13)-XL(14))
XN(4)=XL(11)*(1-XN(1)-XN(2)-XN(3)-XN(5)-XN(6)-XN(7))/(1-XL(8)-
1XL(9)-XL(10)-XL(12)-XL(13)-XL(14))
XN(5)=XL(12)*(1-XN(1)-XN(2)-XN(3)-XN(4)-XN(6)-XN(7))/(1-XL(8)-
1XL(9)-XL(10)-XL(11)-XL(13)-XL(14))
XN(6)=XL(13)*(1-XN(1)-XN(2)-XN(3)-XN(4)-XN(5)-XN(7))/(1-XL(8)-
1XL(9)-XL(10)-XL(11)-XL(12)-XL(14))
XN(7)=XL(14)*(1-XN(1)-XN(2)-XN(3)-XN(4)-XN(5)-XN(6))/(1-XL(8)-
1XL(9)-XL(10)-XL(11)-XL(12)-XL(13))
XNEW1=XN(I)
IF(ABS(XOLD1-XNEW1).LE.0.000001) GO TO 171
GO TO 170
CONTINUE
WRITE(22,204)
FORMAT(16X,1HO,3X,'XLC',6X,'XLMn',5X,'XLSi',5X,'XLNi',5X,'XLCr'
1,5X,'XLMo',5X,'XLCu')
WRITE(22,205)(XL(I),I=1,7)
FORMAT(16X,1HO,7(F8.6,1X)/)
WRITE(22,206)
FORMAT(16X,1HO,3X,'X1C',6X,'X1Mn',5X,'X1Si',5X,'X1Ni',5X,'X1Cr'
1,5X,'X1Mo',5X,'X1Cu')
WRITE(22,207)(XL(I),I=8,14)
FORMAT(16X,1HO,7(F8.6,1X)/)
WRITE(22,172)
```

```
FORMAT(16X,1H0,3X,'XNC',6X,'XNMn',5X,'XNSi',5X,'XNNi',5X,'XNCr'
1,5X,'XNMO',5X,'XNCU')
WRITE(22,173)(XN(I),I=1,7)
FORMAT(16X,1H0,7(F8.6,1X)/)
VLALPH=(X2-XN(1))/(XL(8)-XN(1))
VMTNST=1.-X(15)
TIME,VMTNST,VLMNST
WRITE(22,190)
FORMAT(16X,1H0,2X,'Valpha',5X,'VLalpha',6X,'VMTNST',6X,'VLMNST',
18X,'AC')
WRITE(22,191)X(15),VLALPH,VMTNST,VLMNST,AC
FORMAT(16X,1H0,5(F8.6,4X)/)
CLOSE(UNIT=22,FILE='COM.DAT')
CONTINUE
STOP
END
```